The homeodomain factor Gbx1 is required for locomotion and cell specification in the dorsal spinal cord

Dorsal horn neurons in the spinal cord integrate and relay sensory information to higher brain centers. These neurons are organized in specific laminae and different transcription factors are involved in their specification. The murine homeodomain Gbx1 protein is expressed in the mantle zone of the spinal cord at E12.5-13.5, correlating w ith the appearance of a discernable dorsal horn around E14 and eventually defining a narrow layer in the dorsal horn around perinatal stages. At postnatal stages, Gbx1 identifies a specific subpopulation of GABAergic neurons in the dorsal spinal cord. We have generated a loss of function mutation for Gbx1 and analyzed its consequences during spinal cord development. *Gbx1* -/- mice are viable and can reproduce as homozygous null mutants. However, the adult mutant mice display an altered gait during forward movement, that specifically affects the hindlimbs. This abnormal gait was evaluated by a series of behavioral tests, indicating that locomotion is impaired, but not muscle strength or motor coordination. Molecular analysis showed that the development of the dorsal horn is not profoundly affected in *Gbx1-/-* mutant mice. However, analysis of terminal neuronal differentiation revealed that the number of GABAergic inhibitory interneurons in the superficial dorsal horn is diminished. Our study unveiled a role for *Gbx1* in specifying a subset of GABAergic neurons in the dorsal horn of the spinal cord involved in the control of posterior limb movement.

2   **The homeodomain factor Gbx1 is required for locomotion and cell**

3   **specification in the dorsal spinal cord**

4   Hamid Meziane [1] [*], Valérie Fraulob [2] [*], Fabrice Riet [1], Wojciech Krezel [2], Mohammed Selloum [1],

5   Michaela Geffarth [3], Dario Acampora [4], Yann Hérault [1], Antonio Simeone [4], Michael Brand [3] [#],

6   Pascal Dollé [2] [#] and Muriel Rhinn [2] [#] [@]

7   [1] Mouse Clinical Institute/Institut Clinique de la Souris (MCI/ICS), PHENOMIN, GIE CERBM,

8   1 rue Laurent Fries, 67404 Illkirch Cedex, France

9   [2] Institut de Génétique et de Biologie Moléculaire et Cellulaire, Centre National de la Recherche

10   Scientifique (UMR 7104), Institut National de la Santé et de la Recherche Médicale (U 964),

11   Université de Strasbourg, 1 rue Laurent Fries, 67404 Illkirch Cedex, France

12   [3] DFG-Center for Regenerative Therapies / Cluster of Excellence (CRTD), and Biotechnology

13   Center, Technische Universität Dresden, Fetscherstr. 105, 01307, Dresden, Germany

14   [4] Institute of Genetics and Biophysics "A. Buzzati Traverso" CNR; Via P. Castellino 111, 80131, Naples

15   and   CEINGE   Biotecnologie   Avanzate   Via   G.   Salvatore,   482

16   80145 Naples, and SEMM European School of Molecular Medicine – Naples site

17   Key words: spinal cord, Gbx genes, GABAergic neurons, locomotion, mouse mutant

18   Running title: Phenotypic analysis of *Gbx1^{-/-}* mouse mutants

19   [*] These authors have equally contributed to this study

20   [#] Senior authors

21   [@] Correspondence should be addressed to: Muriel Rhinn (Tel: +33 388 653 342; Fax: +33 388

22   653 201; E-mail: rhinn@igbmc.fr)

23 **Abstract**

24 Dorsal horn neurons in the spinal cord integrate and relay sensory information to higher brain

25 centers. These neurons are organized in specific laminae and different transcription factors are

26 involved in their specification. The murine homeodomain Gbx1 protein is expressed in the

27 mantle zone of the spinal cord at E12.5-13.5, correlating with the appearance of a discernable dorsal horn

28 around E14 and eventually defining a narrow layer in the dorsal horn around perinatal stages. At postnatal stages, Gbx1 identifies

29 a specific subpopulation of GABAergic neurons in the dorsal spinal cord. We have generated a loss of function mutation for Gbx1

30 and analyzed its consequences during spinal cord development. *Gbx1-/-* mice are viable and can reproduce as

31 homozygous null mutants. However, the adult mutant mice display an altered gait during forward movement, that

32 specifically affects the hindlimbs. This abnormal gait was evaluated by a series of behavioral tests, indicating that

33 locomotion is impaired, but not muscle strength or motor coordination. Molecular analysis showed that the development of the dorsal

34 horn is not profoundly affected in *Gbx1-/-* mutant mice. However, analysis of terminal neuronal differentiation revealed that the proportion of

35 GABAergic inhibitory interneurons in the superficial dorsal horn is diminished. Our study unveiled a role for *Gbx1* in specifying a subset of

36 GABAergic neurons in the dorsal horn of the spinal cord involved in the control of posterior limb movement.

Introduction

Perception of sensory inputs from both external and internal environments requires multiple levels of organization in the nervous system. The dorsal spinal cord plays critical roles in organizing responses to sensory input, and contains neurons that relay somatosensory information from sensory neurons in the periphery to motor neurons located in the ventral horns and to higher brain centers (for review: Helms & Johnson 2003). These functions reside in a large number of distinct interneuron types that are arranged in an organized laminar structure in the dorsal horns (Rexed 1952; Brown 1981). Five parallel layers (laminae) have been defined in the murine spinal cord dorsal horn. These laminae are formed of unique combination of neurons, distinguished by their morphology and projections and by their gene expression profiles. The laminae receive different sensory input, with tactile perception mediated by myelinated axon bundles projecting to internal dorsal laminae (III, IV, V), and pain and temperature conveyed through unmyelinated axons that project to more superficial laminae (I, II) (for review: Caspary & Anderson 2003). Proprioception is mediated by sensory neurons that project through the dorsal spinal cord to an intermediate zone which in turn projects to the ventral spinal cord where a direct connection is made with motoneurons (Brown, 1981; for review: Caspary & Anderson 2003).

There are six early-born (in the mouse, by embryonic day E10-12.5) dorsal neuron populations called dI1-dI6 and two late-born (E11-E13) populations called dILA and dILB, defined by expression of specific homeodomain transcription factors (for review: Helms & Johnson 2003, Lewis 2006). These neurons can be further classified by their dependance on roof plate signaling for formation: class A (dI1-dI3) neurons depend on, whereas class B (dI4-dI6, dILA/B) neurons are independent of roof plate signals (Gross, Dottori & Goulding 2002; Müller *et al.* 2002; for review: Helms & Johnson 2003). The dorsal interneuron subtypes dI1-3 migrate ventrally, whereas a subset of dI4 and dI5 cells migrate laterally to populate the deep dorsal horn (laminae IV-V). The dILA/B subclasses migrate to the superficial dorsal laminae (I-III), and mediate pain and temperature sensitive circuits (for review: Caspary & Anderson 2003).

The functional architecture of the mature dorsal horn is the result of developmental processes that involve cell-type specification and differentiation, as well as cell migration. Several events that control the specification of various neuronal subtypes in the spinal cord have been defined in recent studies (for reviews: Lee & Jessell 1999; Briscoe & Ericson, 1999; Caspary & Anderson

68   2003; Lewis 2006). These studies demonstrate that homeodomain transcription factors play a

69   central role during development of neurons in the dorsal horn (for reviews: Goulding *et al.* 2002;

70   Helms & Johnson 2003). Relatively few direct correlations have been made between dorsal

71   interneuron progenitor classes and terminally differentiated cell types. However, formation of the

72   proprioceptor pathway, which projects through the dorsal horn to the ventrally located motor

73   neurons (Brown 1981; Willis & Coggeshall 1991) was shown to be dependent on Math1

74   (Bermingham *et al.* 2001; Gowan *et al.* 1991). Also, a dorsal horn-specific transcription factor, Drg11, is

75   expressed in late born cells derived from dl5 precursors and is required for correct afferent fiber projections of nociceptive

76   sensory neurons and correct dorsal horn morphogenesis (Chen *et al.* 2001; Rebelo *et al.* 2010). Finally, the *Lbx1* gene is

77   required for maturation of several dorsal horn cell types which later populate laminae I-III, and is critical for the correct

78   projection of the nociceptive fibers into these laminae (Gross, Dottori & Goulding 2002; Müller *et al.* 2002).

79   The gene encoding the homeodomain factor Gbx1 is expressed broadly in the mantle zone

80   of the spinal cord at E12.5-13.5 (Rhinn *et al.* 2004 ; Waters *et al.* 2003 ; John, Wildner & Britsch 2005).

81   With the appearance of a discernable dorsal horn around E14, *Gbx1* expression becomes more restricted, eventually defining a

82   narrow layer in the dorsal horn around perinatal stages (John, Wildner & Britsch 2005). Recently, immunohistological analysis

83   showed that at E12.5, only a subpopulation of the Lbx1-positive cells coexpress Gbx1 (John, Wildner & Britsch 2005). Lbx1 is a key

84   determinant for the specification of class B neurons (Gross, Dottori & Goulding 2002; Müller *et al.* 2002), suggesting that

85   Gbx1-positive cells could correspond to class B neuron precursors (John, Wildner & Britsch 2005). Late-born class B neurons comprise

86   initially two neuron populations, dILA and dILB, which are born in an apparent salt and pepper pattern in the dorsal spinal cord.

87   dILA neurons express *Lbx1*, *Pax2*, and *Lhx1/5*, whereas dILB cells express *Lbx1*, *Lmx1b*, and *Tlx3* (Müller *et al.* 2002). At E12.5

88   and E14.5, Gbx1 neurons co-express the transcription factors Lhx1/5 and Pax2, but are negative for Lmx1b and Tlx3. This

89   indicates that Gbx1 expression distinguishes a subpopulation of dILA neuronal cells (John, Wildner & Britsch 2005). Furthermore, these

90   authors show that GABA or Gad67 expressing neurons coexpress Gbx1, suggesting that Gbx1-positive cells may differentiate into

91   GABAergic neurons.

92   To investigate the function of Gbx1 during dorsal horn development, we have generated mice bearing a mutation that ablates

93   Gbx1 function. We report that *Gbx1* knockout mice are viable and can reproduce as homozygous null mutants.

94   However, the adult mutant mice display an altered gait during forward movement that specifically affects hindlimbs.

95   This abnormal gait was evaluated by a series of behavioral tests, which revealed that locomotion is impaired, but not muscle

96   strength or motor coordination. We then analyzed the development of the spinal cord dorsal horn in *Gbx1*-/- mice. Despite the clear

97   behavioral phenotype, we did not observe changes in the expression of homeodomain factors regulating dorsal spinal cord development,

98   suggesting that development of the dorsal horn is not profoundly affected in *Gbx1*-/- mice. However, analysis of terminal neuronal differentiation

99   revealed that expression of *Gad67,* a marker for GABAergic inhibitory interneurons, is diminished. Gbx1 is therefore required for the

100   differentiation of inhibitory local circuit interneurons in the superficial dorsal horn, demonstrating a function for this transcription factor in the

101   dorsal horn of the spinal cord.

102   Materials and methods

103   Construction of a *Gbx1* targeting vector

104   Genomic sequences encompassing the mouse *Gbx1* gene were isolated from a 129SV genomic phage library, using as a probe a

105 *Gbx1* cDNA fragment previously characterized (Rhinn *et al.* 2004). A *Gbx1* loss of function mutation was produced by homologous
106 recombination in embryonic stem cells (Ramìrez-Solis, Davis & Bradley 1993). The targeting vector contained a 5.4 kb *Xmn*I fragment
107 (upstream arm), ending 33 bp upstream of the homeodomain sequence located in *Gbx1* second exon, and a 1.6 kb *Kpn*I fragment
108 (downstream arm), whose sequence started 91 bp downstream from the homeodomain. These fragments were excised from the
109 recombinant phage and cloned in the mutagenesis pGN vector (Le Mouellic, Lallemand & Brûlet 1990) to generate the pGN-
110 *Gbx1* targeting vector (Fig. 1A). In this vector, the fragments are inserted on each side of a *lacZ* reporter gene and a neomycin
111 resistance gene, and their insertion by homologous recombinaton in the *Gbx1* gene will generate a 313 bp deletion encompassing the
112 entire homeodomain (Fig. 1A).

113 **Transfection of embryonic stem cells and selection of targeted clones**
114 HM-1 embryonic stem (ES) cells (Magin, Whir & Melton 1992) were cultured on neomycin-resistant mouse embryonic
115 fibroblasts, as described in Robertson, 1987. Ten μg of the pGN-*Gbx1* targeting vector were linearized by digestion of the unique
116 *Not*I restriction site, and electroporated into 2×10^7 ES cells resuspended in 750 μl HeBS medium (20 mM Hepes pH 7.05, 137 mM
117 NaCl, 5 mM KCl, 0.7 mM Na_2HPO_4, 6 mM glucose), at 200 V, 960 μF. Positive selection was carried out for 11 days with 350
118 μg/ml G418. Resistant colonies were picked and DNA was extracted from a fraction (1/5) of the cells to perform Southern blot
119 analysis to identify homologous recombination events. The probe used is an external fragment located immediately downstream
120 to the targeting vector (Fig. 1A,B). Positive clones were expanded before freezing. The frequency of homologous
121 recombination was 7 out of 350 clones analyzed.

122 **Generation and genotyping of chimeric and mutant mice**
123 After thawing, 10 to 15 ES cells were microinjected into blastocysts collected at E3.5 from C57BL/6 females mated with
124 C57BL/6 males (for procedures: Nagy *et al.* 2003). Injected blastocysts were reimplanted in the uterine horn of pseudopregnant
125 recipient females. Chimeric animals were back-crossed to C57BL/6J mice and germ-line transmission was scored by the presence
126 of agouti coat pigmentation. Heterozygous offspring were identified by PCR genotyping. Tail tips were incubated in lysis buffer
127 (50 mM Tris pH 8.0, 100 mM EDTA, 100 mM NaCl, 1% SDS, 0.6 mg/ml proteinase K) overnight at 55°C, phenol-chloroform
128 extracted, ethanol precipitated and redissolved in 10 mM Tris-HCl, 1 mM EDTA pH 8.0 at a final concentration of 0.2-1.0 μg/μl.
129 The presence of a wild-type or mutated allele was detected using three primers: a sense primer F1: 5'-
130 GGTGACAGCGAGGACAGCTTCCT-3', an antisense primer R1: 5'-CCCAGAACGACTGCTCACATTGC-3', and an antisense
131 primer LacZ R2: 5'-GGCCTCTTCGCTATTACGCCA-3'. The presence of a wild-type allele was detected using the F1/R1
132 primers which amplify a 354 bp fragment. The presence of a mutated allele was detected by using the F1/LacZ R2 primers which
133 amplify a 269 bp fragment. Thirty cycles (denaturation: 1 min, 95°C, annealing : 1 min, 62°C; elongation : 30 s, 74°C) were
134 performed, and the amplified products were separated by 2% agarose gel electrophoresis (Fig. 1C). Phenotypic and
135 molecular analyses were performed after several generations of backcrosses (>5) to C57BL/6J mice,
136 resulting in a nearly pure genetic background.

137 **Tissue collection and sample preparation**
138 Pregnant females obtained from natural matings (morning of vaginal plug was considered as E0.5) were sacrificed and fetuses
139 were collected in phosphate-buffered saline (NaCl: 8.01 g/L, KCl: 0.2 g/L, Na_2HPO_4, $2H_2O$: 1.78 g/L, KH_2PO_4: 0.27 g/L, pH 7.5;
140 hereafter abbreviated PBS 1x) after cesarean section. The specimens were dissected, fixed overnight in 4% paraformaldehyde (PFA) diluted in
141 PBS 1x, pH 7.5, cryoprotected in 20% sucrose in PBS 1x, pH 7.5 and embedded in Shandon Cryomatrix (Thermo Electron Corperation) before freezing
142 at -80°C. Cryosections (14 μm thickness, Leica CM3050S cryostat) sections were made in a coronal plane, collected on Superfrost slides, and
143 stored at -80°C until use.

144   For whole-mount immunostaining or in situ hybridization, embryos were fixed overnight in 4% PFA, dried at room temperature, and stored at -20
145 °C in 100% methanol.

146 **In situ hybridization**

147 In situ hybridization was performed with digoxigenin-labeled probes as previously described
148 (Chotteau-Lelièvre *et al.* 2006). Template DNAs were kindly provided by Drs K. Jagla (*Lbx1*), C.
149 Birchmeier (*Lmx1b*), M. Tessier-Lavigne (*Netrin*), A.J. Tobin (*Gad67*) and P. Gruss (*Pax2*), P.
150 Bouillet (*Gbx2*), B. Giros (*Slc17a6*), F. Chen (*Drg11*), R. Krumlauf (*Hoxb1*), and F. Rijli
151 (*Hoxa2*). For all experiments 3 animals of each genotype, from 2 or more independent litters,
152 were analyzed (except for *Gbx2*: Fig. S1A-D, n=2). Cell countings were performed in the dorsal
153 horn (*Gad67*, *Pax2*, *Slc17a6*) or ventral horn (Islet1) on 3 transverse sections for each animal, at
154 comparable levels of the lumbar spinal cord (all sections were collected serially, with section
155 planes being separated by 112 μm). Three animals of each genotype were thus analyzed for each
156 marker.

157   All expression patterns were documented using a macroscope (Leica M420) or microscope (DM4000B, objective 10x),
158 both connected to a Photometrics camera with the CoolSNAP (v. 1.2) imaging software (Roger Scientific, Chicago, IL). Cell
159 counts were performed using the image J (NIH 1.45S) software. Blue labelled cells and
160 unlabelled cells were counted manually with the cell counter plugin. Three sections separated by
161 112 μm in 3 independent embryos were counted for each condition, and statistical significance of
162 cell counts was validated with a two way measures analysis of variance (ANOVA) with the first variable as fixed
163 effect (i.e. genotype) and a second variable as random effect of repeat observations on the same individual. The level of
164 significance was set at p<0.05. Graphs represent averages of counting values and SEM.

165 **Immunohistochemistry**
166 After antigen unmasking in citrate buffer 0.01 M (pH 6) during 15 min in a microwave oven, sections were treated in H_2O_2 3% in PBS 1x, pH 7.5 for 5 min,
167 rinsed in PBS 1x, then blocked in PBS 1x, pH 7.5 containing 0.25% Triton-X100, 5% normal goat serum and incubated overnight at 4°C with rabbit anti-
168 Gbx1 (kindly provided by Dr S. Britsch; 1:500), rabbit anti-calbindin D-28K (Chemicon, 1:1000), rabbit anti-Peripherin (Chemicon, 1:500), or mouse anti-Islet1 (40.2D6,
169 concentrated, Developmental Studies Hybridoma Bank, Iowa City, IA, 1:100) in PBS 1x, pH 7.5 containing 0.25% Triton-X100, 5% normal goat serum
170 followed by species-specific biotin-coupled secondary antibodies (1:400, Jackson Laboratories) diluted in PBS 1x, pH 7.5. Detection was performed
171 using a Vectastain Elite ABC Kit, following the manufacturer's instructions. Nissl staining was performed by incubation in 0.5% cresyl violet in water for 15 min.
172 TUNEL was performed using the APOPTAG® Peroxidase In Situ Apoptosis detection kit (Millipore). For all
173 experiments 3 animals of each genotype were analyzed.

174 **Behavioral phenotyping procedures**
175 Cohorts of 10 week-old male and female *Gbx1-/-* mice in a C57BL/6J genetic background (7 males and 8 females), with their
176 wild-type (WT, 10 males and 9 females) counterparts, were used in this study. Mice were group housed and allowed 2 weeks
177 acclimation in the phenotyping area with controlled temperature (21-22°C) under a 12-12 h light-dark cycle (lights on 7am-7pm),

178 with food and water available ad libitum. Testing started at 10 weeks of age, and all procedures were carried out in accordance
179 with European institutional guidelines. Behavioral tests were performed successively for each cohort of mice, during the light
180 phase of the circadian cycle, according to a pipeline established by the European Mouse Disease Clinic (EUMODIC pipeline 2),

181 by trained experimenters familiar with observation of normal gait patterns in mice. Detailed
182 procedures for each test are available at the URL: http://www.empress.har.mrc.ac.uk/viewempress/index.php?
183 pipeline=EUMODIC+Pipeline+2.

184 *Neurological examination:* General health and basic sensory motor functions were evaluated using a modified SHIRPA protocol
185 (Brown, Chambon & Hrabé de Angelis 2005; protocol at http://www.empress.har.mrc.ac.uk/viewempress/index.php?
186 pipelineprocedure=EUMODIC+Pipeline+2~Modified+SHIRPA). This analysis is adapted from the procedure developed by Irwin
187 (1968) and from the SHIRPA protocol (Hatcher *et al.* 2001). It provides an overview of physical appearance, body weight,
188 neurological reflexes and sensory abilities.

189 *Rotarod test:* This test evaluates motor coordination and balance by measuring the ability of animals to maintain balance on a
190 rotating rod (Bioseb, Chaville, France). Mice were given three testing trials during which the rotation speed accelerated from 4 to
191 40 rounds per min (rpm) over 5 min. Trials were separated by 5-10 min intervals. The average latency (time to fall from the
192 rotating rod) of the three trials was used as index of motor coordination performance.

193 *Grip test:* This test measures the maximal muscle strength (g) using an isometric dynamometer connected to a grid (Bioseb). Mice
194 were allowed to grip the grid either with the forepaws or with both the forepaws and hindpaws, then were pulled backwards until
195 they released the grid. Each mouse was submitted to 3 consecutive trials immediately after the modified SHIRPA procedure. The
196 maximal strength developed by the mouse before releasing the grid was recorded and the average value of the three trials was
197 adjusted to body weight.

198 *Beam walking:* This test is used to evaluate fine motor coordination and proprioceptive function. The apparatus used is a 2 cm
199 diameter and 110 cm long wooden beam, elevated 50 cm above the ground. A goal box (12 x 12 x 14 cm) is attached at one
200 extremity of the beam. Animals were first habituated to the goal box for 1 min. They were then submitted to 3 training trials
201 during which they were placed at different points of the beam, with the head directed to the goal box, and allowed to walk the
202 corresponding distance to enter the goal box.

203 After training, animals were submitted to 3 testing trials during which they were placed at the extremity of the beam opposite to
204 the goal box and allowed to walk the beam distance and enter the goal box. The latency to enter the goal box and the number of
205 slips (when one or both hindpaws slipped laterally from the beam) were measured.

206 *Hot plate test:* The mice were placed into a glass cylinder on a hot plate (Bioseb) adjusted to 52°C, and the latency of the first
207 pain reaction of any hindlimb (licking, flinches) was recorded, with a maximum of 30 s testing.

208 *Electrophysiological measurements:* Electrophysiological recordings were performed under ketamine-xylazine anesthesia (100
209 and 10 mg/kg body weight, respectively) using a Key Point electromyograph apparatus (Medtronic, France). Disposal scalp
210 needle electrodes were used (ref 9013R0312, Medtronic). The body temperature was maintained at 37°C with a homeothermic
211 blanket (Harvard, Paris, France). For measuring the sensory nerve conduction velocity (SNCV), recording electrodes were
212 inserted at the proximal part of the tail and stimulating electrodes placed 20 mm from the recording needles towards the extremity
213 of the tail. A ground needle electrode was inserted between the stimulating and recording electrodes. Caudal nerve was stimulated
214 with a series of 20 pulses of 0.2 ms duration at a supramaximal intensity of 8 mA. The average response is included for statistical
215 analysis. The compound muscle action potential (CMAP) was measured in gastrocnemius muscle after sciatic nerve stimulation.
216 For this purpose, stimulating electrodes were placed at the level of the sciatic nerve at 1 cm from the vertebral column, and
217 recording electrodes placed in the gastrocnemius muscle. A ground needle was inserted in the contralateral paw. The sciatic nerve
218 was stimulated with a single 0.2 ms pulse at a supramaximal intensity of 8 mA. The amplitude (mV) and the distal latency of the
219 responses (ms) were measured.

220 ***Anxiety-related behavior - open field test:*** Mice were tested in automated open fields (Panlab, Barcelona, Spain), each virtually
221 divided into central and peripheral regions. The open fields were placed in a room homogeneously illuminated at 150 Lux. Each
222 mouse was placed in the periphery of the open field and allowed to explore freely the apparatus for 20 min, with the experimenter
223 out of the animal's sight. The distance traveled, the number of rears, and time spent in the central and peripheral regions were
224 recorded over the test session. The latency and number of crosses into as well as the percent time spent in center area are used as
225 index of emotionality/anxiety.

226 ***Sensorimotor gating - auditory startle reflex reactivity and pre-pulse inhibition (PPI):*** Acoustic startle reactivity and pre-pulse
227 inhibition of startle were assessed in a single session using standard startle chambers (SR-Lab Startle Response System, San
228 Diego Instruments). Ten different trial types were used: acoustic startle pulse alone (110 db), eight different prepulse trials in
229 which either 70, 75, 85 or 90 dB stimuli were presented alone or preceding the pulse, and finally one trial (NOSTIM) in which
230 only the background noise (65 dB) was presented to measure the baseline movement in the Plexiglas cylinder. In the startle pulse
231 or prepulse alone trials, the startle reactivity was analyzed, and in the prepulse plus startle trials the amount of PPI was measured
232 and expressed as percentage of the basal startle response.

233 ***Statistical analyses:*** Data were analyzed using unpaired Student t-test, one way or repeated measures analysis of variance
234 (ANOVA) with one between factor (genotype) and one within factor (time). Qualitative parameters (i.e. some of the clinical
235 observations) were analyzed using χ^2 test. The level of significance was set at $p<0.05$.

Animal ethics statement

237 Animal experimentation protocols were reviewed and approved by the Direction Départementale
238 des Services Vétérinaires (agreement #67-172 to H.M., 67-189 to P.D., and institutional
239 agreement #D67-218-5 for animal housing) and conformed to the NIH and European Union
240 guidelines, provisions of the Guide for the Care and Use of Laboratory Animals, and the Animal
241 Welfare Act.

Results and discussion

Gbx1-deficient mice are viable, but display a typical duck-like gait

244 A loss of function allele for the *Gbx1* gene was generated by homologous recombination in murine embryonic stem cells (see Materials and
245 Methods). The mutated *Gbx1* allele is devoid of the entire homeodomain-coding sequence and ~100 adjacent nucleotides (Fig. 1A-C). After
246 generation of germ-line transmitting chimeras, heterozygous mutant mice (*Gbx1*+/-) were found to be viable, fertile and apparently normal. After
247 intercrossing *Gbx1*+/- mice, *Gbx1*-/- mutants (generated in a C57BL/6J genetic background) were born in the expected mendelian ratio.
248 Immunohistochemistry performed with an anti-Gbx1 antibody confirmed the absence of detectable Gbx1 protein in the spinal cord of E18.5
249 *Gbx1*-/- mutants (Fig. 1D,E). We also checked the expression of *Gbx2* from E12.5 to E18.5 (Fig. S1) to exclude a potential compensatory
250 expression due to the loss of function of *Gbx1*. A subtle increase of *Gbx2* mRNA expression might occur in spinal cord cells of *Gbx1*-/- mice at
251 E12.5-14.5, however this increase was no longer detected at E16.5 or E18.5 (Supplementary material, Fig. S1). This subtle *Gbx2* increase could
252 partially compensate for the loss of Gbx1, leading to the absence of phenotypic abnormalities at early developmental stages. Interestingly, when
253 observed by 10 weeks of age, most mutants displayed a typical, unevenness in walking ("duck-like") gait (Fig. 2 and Supplementary material:
254 movie). Both male and female *Gbx1*-/- mice were fertile and had a normal life span.

255 **General health and sensorimotor abilities in adult *Gbx1* mutants**

256   *Gbx1-/-* males and females had a normal body weight (Table 1) and a normal overall physical appearance. However, many of the *Gbx1-/-* mutants

257   showed significantly abnormal gait (χ^2 ≥5.20, p<0.05). Indeed, 43% of *Gbx1* mutant males and 63% of *Gbx1* mutant females displayed lack of

258   fluidity in movement, and limping related to hyper-flexion followed by hyper-extension of one or both hindpaws (Table 1; Fig. 2; Supplementary

259   material: movie). *Gbx1-/-* males and females also showed significantly reduced short-term locomotor activity following immediate transfer for the

260   modified SHIRPA test, as compared to WT counterparts (t≥3.46, p<0.01) (Table 1). The other features of general health and basic neurological

261   reflexes were not affected in *Gbx1* mutants.

262   When tested for specific motor abilities, motor coordination performance measured in the rotarod test (t≤1.29, NS) and the muscle strength

263   (grid grip) test (t≤1.38, NS) were not affected in *Gbx1-/-* males and females (Table 1). In the beam walking test, the latency to cross the beam was

264   increased (t_{15}=3.71, p<0.01 for females; non significant for males) and the number of slips was slightly increased (even if not significantly),

265   especially in *Gbx1-/-* females (Fig. 3). In the open field test, there was a significant effect of genotype concerning locomotor activity

266   [F(1,30)=6.51, p<0.05], reflecting reduced locomotion in all *Gbx1-/-* animals. When considering each gender separately, both *Gbx1-/-* males and

267   females tended to have reduced locomotor activity over the testing period (although not statistically significant, p=0.09) (Fig. 4). The average

268   speed during motion was also significantly lower in *Gbx1-/-* males and females than in WT (t≥3.36, p<0.01) (Fig. 4). The number of entries into,

269   and the percentage of time spent in, the center of the arena also differed between genotypes [F(1,30)≥14.48, p<0.001]. Both *Gbx1-/-* males and

270   females had significantly decreased number of entries and spent less time in the center of the open field than WT counterparts (t≥2.62, p<0.05)

271   (Fig. 4), which might reflect increased anxiety in *Gbx1-/-* mutants. The reduced exploration of the center might also be due to the observed

272   reduced locomotor activity of *Gbx1-/-* mutants. Altogether, these data show that *Gbx1-/-* mutant mice have a clear defect in locomotion, although

273   this defect does not appear to result from a coordination problem or a muscle strength deficiency.

274   To test whether ablation of Gbx1 could affect sensory response, we measured the response of *Gbx1* mutant mice in a hot plate test. The

275   withdrawal latency was higher in *Gbx1-/-* males (but not in females) than in WT (t_{15}=2.10, p=0.05) (Table 1), suggesting reduced thermal pain

276   sensitivity in *Gbx1* mutant males.

277   The consequence of *Gbx1* inactivation on acoustic startle and pre-pulse inhibition of startle reflex was also evaluated. Regardless of gender,

278   the startle reactivity was comparable between WT and *Gbx1-/-* mice for all the acoustic stimuli including the startling pulse [Genotype

279   F(1,30)≤0.83, Sex F(1,30)≤0.85, Genotype*Sex F(1,30)≤1.11, NS] (Fig. 5). When the startling pulse was preceded with prepulses with lower

280   intensities, the PPI level was also comparable between genotypes [Genotype F(1,30)=0.55, Sex F(1,30)=0.32, Genotype*Sex F(1,30)=0.11, NS)]

281   (Fig. 5). Furthermore, electromyography (EMG) measurements revealed that the sensory nerve conduction velocity (SNCV) differed significantly

282   between genotypes [F(1,29)=7.31, p<0.05]; indeed, *Gbx1-/-* females had significantly increased SNCV (t_{14}=2.83, p<0.05) (Table 2), as measured

283   at the level of the caudal nerve. On the other hand, the latency and amplitude of the gastrocnemius muscle response evoked by sciatic nerve

284   stimulation were comparable between genotypes [F(1,29)=1.63, NS].

285   In summary, we used a variety of behavioral and electrophysiological phenotyping tests to evaluate sensory and motor functions in

286   *Gbx1* mutant mice. Decreased exploratory behavior was found in the open field test and following immediate transfer during clinical observations.

287   Exploration of the central part of the open field arena was significantly decreased in *Gbx1-/-* males and females, which might suggest increased

288   anxiety in these mutants. However, this could also be due to the reduced locomotor activity of the mutants. Indeed, *Gbx1-/-* mice also showed

289   decreased average speed with no significant effect on the distance travelled in the open field. Their altered gait during forward movement might

290   explain the reduced speed and locomotor activity in the open field, which could not be attributed to defects in motor coordination or muscle

291   strength. Abnormal gait may suggest proprioceptive-like deficits, as indicated by abnormal performance in beam walking, the test used for

292   evaluation of proprioceptive functions, which was statistically significant only for *Gbx1-/-* females. Although no direct link can be clearly

293   identified between motor deficits and sensory functions, we cannot exclude mutual interdependence of abnormal gait and sensory deficits

294   indicated by reduced responses in hot plate test and increased SNCV, which were penetrant to a different degree in null-mutant males and females.

295   ***Gbx1-/- mice do not show obvious hindbrain patterning defects***

296   *Gbx* genes are related to the Drosophila *unplugged* gene, which acts during development of the tracheal system, and for

297   specification of neuroblast sublineages (Chiang *et al.* 1995; Cui & Doe 1995). There are two *Gbx* genes in amniote species

298   (human, mouse and chicken), as well as in zebrafish (Lin *et al.* 1996; Bouillet *et al.* 1995; Shamim & Mason 1998; Niss &

299   Leutz 1998; Rhinn *et al.* 2003). Previous studies showed that in mouse, *Gbx2* is involved in early specification of the midbrain-

300   hindrain boundary (MHB) organizer, a signaling center that will pattern the anterior hindbrain rhombomeres (Wassarman *et*

301   *al.* 1997; Waters & Lewandoski 2006; for review: Rhinn & Brand 2001; Simeone 2000). In zebrafish it was shown

302 that *gbx1* acts during early positioning of the MHB, whereas *gbx2* functions at later stages, once the MHB is established (Rhinn *et*
303 *al.* 2004; 2009; Burroughs-Garcia *et al.* 2011). In mouse, *Gbx1* is not expressed at the MHB as is the case during early zebrafish
304 development. Its expression starts at E7.75 in the prospective hindbrain, spanning rhombomeres 2 to 7 during the segmentation
305 phase (Rhinn *et al.* 2004; Waters, Wilson & Lewandoski 2003). This suggested that *Gbx1* might be
306 involved in early embryonic hindbrain patterning, which could underlie behavioral deficits
307 associated with loss of Gbx1 function. To assess for possible rhombomeric abnormalities in
308 *Gbx1*-/- mutants, we performed whole-mount in situ hybridizations at E9.5 with several markers,
309 including *Hoxb1* and *Hoxa2*. This analysis did not show any molecular or structural abnormality
310 of the hindbrain rhombomeres in *Gbx1*-/- embryos (Supplementary material, Fig. S2). This suggests
311 that Gbx1 is not required for early hindbrain patterning, in contrast to its mouse homologue Gbx2
312 (Wassarman *et al.* 1997; Waters & Lewandoski 2006). Analysis of hindbrain derivatives (brain
313 stem and cerebellum) at E18.5 using *Gad67* as a differentiation marker also did not reveal any
314 difference in *Gbx1*-/- versus wild-type mice (Supplementary material, Fig. S3).

315 **Development of the spinal cord dorsal horn in *Gbx1* mutant mice**
316 At E12.5, the expression domains of *Gbx1* and *Gbx2* overlap, both being expressed in the ventricular and mantle zones of the
317 dorsal spinal cord (Rhinn *et al.* 2004; Waters, Wilson & Lewandoski 2003). As *Gbx2* expression is downregulated
318 after E12.5, both genes are only transiently coexpressed in dorsal spinal cord progenitor cells, and *Gbx1* is the only *Gbx* gene
319 persistently expressed during later dorsal horn development (John, Wildner & Britsch 2005).
320 Thus, the prominent expression of *Gbx1* in the dorsal horn could be relevant for the abnormal gait
321 phenotype of adult *Gbx1* mutant mice, which led us to ask whether *Gbx1* is required for the
322 maturation and/or specification of neurons of the dorsal horn during development. Nissl staining of E18.5
323 spinal cord sections revealed no obvious difference between the dorsal horn of wild-type and *Gbx1*-/- animals at thoraco-lumbar levels (Fig.
324 6A,B). Despite the clear behavioral phenotype, we were unable to identify any consistent alteration in the expression of several molecular markers
325 of dorsal spinal cord cell populations in *Gbx1*-/- embryos. These markers included the genes encoding the transcription factors *Lbx1* (Gross,
326 Dottori & Goulding 2002; Müller *et al.* 2002) (Fig. 6C,D), *Lmx1b* (Chen *et al.* 2001) (Fig. 6E,F) and the axon guidance molecule
327 *Netrin-1* (Leonardo *et al.* 1997) (Fig. 6G,H) analyzed at E12.5, 14.5, 16.5 and 18.5, and shown (Fig. 6) at E16.5.

328 **Projection pattern of primary sensory afferents in the dorsal horn of *Gbx1*-/- mutants**
329 We examined the development of primary sensory afferent projections to the dorsal horn, which are well defined at E18.5, in *Gbx1* mutant
330 mice. The projections of cutaneous nociceptive sensory neurons begin to invade the spinal grey matter by E12.5 (Ozaki & Snider 1997).
331 Immunostaining with an anti-calbindin-28K antibody at E16.5 and E18.5 marks a subset of cutaneous neurons and their afferent fibers (Honda
332 1995; Chen *et al.* 2001). By E18.5, calbindin+ fibers have invaded the dorsal horn of wild-type and *Gbx1* mutants (Fig. 7A-B'). The *Drg11* gene is
333 required for the projection of cutaneous sensory afferent fibers to the dorsal spinal cord (Chen *et al.* 2001). In *Gbx1*-/- mutant mice, *Drg11*
334 expression was not affected in the dorsal horn at E12.5, 14.5, 16.5 or 18.5 (Fig. 7C,D and data not shown). Altogether, these data suggest that
335 there are no defects in patterning of sensory afferent fiber projections to the dorsal horn, which selectively affects cutaneous afferents, although
336 the markers used cannot rule out other types of patterning differences (for instance
337 from primary afferents that do not label with calbindin).

338   We further examined proprioceptive afferents at E18.5 by using antibodies to peripherin (Escurat *et al.* 1990). No consistent difference
339 between wild-type and *Gbx1-/-* mice was observed at the level of proprioceptive fibers that extend toward motoneurons and interneurons in the
340 deep dorsal horn, or at the level of fibers that enter into the spinal gray matter, at E18.5 (Fig. 7E,F) or E16.5 (Fig. 7G,H). During the revision of
341 our manuscript, another *Gbx1* mutant allele was described (Buckley *et al.* 2013). In contrast to our observations and at a comparable stage, those
342 mutants show disorganized peripherin expression, together with a decrease of Islet1-expressing cells in the ventral horn of the lumbar spinal cord
343 (Buckley *et al.* 2013). This led us to analyze Islet1-expressing cells in ventral motor neurons in our *Gbx1* mutants. No differences in the number of
344 Islet1+ cells within the lumbar ventral spinal cord were found at E14.5, E16.5 (Fig. S4) or E18.5 (data not shown). Thus, in contrast to the data of
345 Buckley *et al.*, our analysis does not suggest a defect in the assembly of the proprioceptive sensorimotor circuit. As the same *Gbx1* exon (exon 2)
346 was targeted in both loss of function alleles, the reason for the phenotypic discrepancy remains unclear, although it should be mentioned that the
347 mice might have different genetic backgrounds.

348   **Reduced GABAergic neuronal differentiation in *Gbx1-/-* mutants**

349 *Gbx1* is first expressed in the ventricular zone of the spinal cord at E11.5 (Rhinn *et al.* 2004 ; Waters, Wilson &
350 Lewandoski 2003). Then at E12.5-E13.5, it is broadly expressed in the mantle zone of the dorsal spinal cord. At E14
351 with the appearance of a distinguishable dorsal horn, *Gbx1* expression becomes more restricted. At E12.5, *Gbx1* is
352 coexpressed with *Lbx1;* thus *Gbx1* cells correspond to class B neurons (John, Wildner & Britsch 2005). As described in the
353 introduction, late-born class B neurons comprise initially two populations, dILA and dILB. Because *Gbx1* neurons co-
354 express *Lhx1/5* and *Pax2,* but not *Lmx1b* and *Tlx3*, it has been suggested that these neurons correspond to the dILA
355 neuronal subtype (John, Wildner & Britsch 2005). It has been shown that dILA neurons undergo GABAergic differentiation
356 (Cheng *et al.* 2004), and as mature GABA+ neurons they continue expressing *Gbx1* (John, Wildner & Britsch 2005). We
357 therefore analyzed GABAergic neurons in the spinal cord of *Gbx1-/-* mutants, which we identified by expression of
358 glutamic acid decarboxylase GAD67, an enzyme that regulates GABA synthesis. At E18.5, *Gad67*-expressing cells are found
359 throughout the developing spinal cord of control mice (Somogyi *et al.* 1995). Importantly, *Gad67* expression was reduced in the dorsal spinal cord
360 of *Gbx1* mutant mice (Fig. 8A-D), i.e. there was a 16% decrease in the proportion of *Gad67*-expressing cells (Fig. 8I). This may reflect an abnormal
361 development of GABAergic neurons, which in consequence coud lead to abnormal control of neuronal network in dorsal horn, possibly affecting
362 inhibitory circuits throughout the spinal cord. This finding was strengthened by analysis of *Pax2*, another gene expressed in GABAergic cells in
363 the spinal cord (Cheng *et al.* 2004), with cell countings corroborating the decrease in the proportion of GABAergic cells (Fig. 8E,F,I).
364 Furthermore, it is know that during early post-natal period, the GABA pathway switches from excitatory to inhibitory in
365 mouse (Ben-Ari *et al.* 2007). This shift was shown to occur within the two first weeks of age in hippocampal and
366 spinal motor neurons in mouse (Stein *et al.* 2004) as well as in lamina I in rats (Sibilla & Ballerini 2009). Also, it was
367 mentioned that the switch depends on the species, sex, brain structures and neuronal types (Ben-Ari *et al.* 2007)
368 and it was shown using a model system of cultured hippocampal neurons that the switch
369 is triggered by GABAergic activity itself (Ganguly *et al.* 2001). Interestingly, when *Gbx1-/-*
370 pups were checked visually around weaning every day in the morning (analysis done on 5 litters, 42 pups, 8 *Gbx1-/-*
371 mutants), the locomotor deficits were first observed around post-natal days (P)16-17. Taking in account an
372 eventual delay due to a diminished GABA activity, the appearance of the
373 locomotion defect could coincide with the time point at which the GABA pathway switches from
374 excitatory to inhibitory.
375 We also observed that *Gad67* expression was unchanged in the brain stem and cerebellum of E18.5 *Gbx1-/-* mutants (Fig.
376 S3), arguing against an involvement of these structures in the observed phenotype.

377   We next addressed the question if the observed decrease of GABAergic cells is due to neuronal cell death or to a
378   possible change of GABAergic to glutamatergic fate. TUNEL experiments were performed at various stages (E12.5, 14.5,
379   16.5, 18.5; Fig. 9 and data not shown). As expected, natural cell death occurs mainly in the developing spinal ganglia and
380   ventral spinal cord (Fig. 9A,B; White *et al.* 1998) and natural cell death is suggested to be over by E15.5 (Fig. 9C,D; White
381   *et al.* 1998). Our analysis showed no abnormal apoptosis in the dorsal spinal cord of *Gbx1*-/- mice (Fig. 9B,D). This
382   finding would exclude that the decrease of *Gad67*-expressing cells is due to cell death, and suggest that Gbx1 is not
383   required for cell survival. We then analyzed expression of *Slc17a6*, encoding VGLUT2, a vesicular glutamate transporter
384   expressed in glutamatergic neurons (Kaneko *et al.* 2002). At E18.5, *Slc17a6*-expressing cells were increased in the dorsal
385   spinal cord of *Gbx1* mutant mice (Fig. 8G,H). This finding suggests that part of the "missing" GABAergic cells may have
386   differentiated into glutamatergic neurons.

387   Glutamate and GABA are the main neurotransmitters for excitatory and inhibitory neurons, respectively, in the vertebrate
388   brain. These neurotransmitters are usually expressed in a mutually exclusive manner (Bellocchio *et al.* 2000; Fremeau *et al.* 2001). In the
389   dorsal horn of the spinal cord, most ascending projection neurons and a subset of local circuit interneurons are excitatory and are
390   glutamatergic. These neurons are modulated by local inhibitory neurons, many of which are GABAergic (for reviews: Melzack &
391   Wall 1965; Malcangio & Bowery 1996; Dickenson 2002). Thus, GABA may inhibit transmitter release from primary afferent fibers. The output
392   neurons of the dorsal horn are projection neurons, relaying sensory information to several brain areas. However, the majority of
393   dorsal horn neurons are local circuit interneurons that do not project outside of the spinal cord. The output of projection neurons is
394   influenced by local excitatory and inhibitory neurons (Todd 2010; Larsson & Broman 2011; Guo *et al.* 2012). In *Gbx1* mutants,
395   the reduction in the proportion of GABAergic neurons, and the possible switch of some of these neurons to a glutamatergic
396   identity, may disrupt neuronal circuitry, becoming phenotypically apparent at adult stages as measured by abnormal performance
397   in several behavioral tests. Further electrophysiological studies will be necessary to link the decrease of GABAergic neurons to
398   the abnormal gait observed in adult *Gbx1* mutant mice.

399   **Conclusion**

400   We have generated *Gbx1*-/- loss of function mutant mice, and investigated the development of the spinal cord dorsal horn in these mutants.
401   *Gbx1*-/- mutants are viable and fertile, but display an altered gait during forward movement that specifically affects
402   hindlimbs, beginning at post-natal days 16-17. This abnormal gait, documented by a series of behavioral tests, is not due
403   to deficits in muscle strength or motor coordination. Although reduced performance of *Gbx1*-/- mice in beam walking, a test used
404   in studies of proprioception, could potentially suggest proprioceptive deficits, such a hypothesis is not fully supported by at least
405   two observations: (i) the incomplete penetrance of this phenotype because significant deficits were observed only in females, and
406   (ii) by molecular data, which did not reveal deficits in the assembly of proprioceptive sensory afferents in the ventral or
407   intermediate zone, described previously (Brown, 1981) as their target regions before contacting motoneurons.

408   Some of the deficits, such as altered sensory nerve conduction velocity, are significantly altered in females, whereas significant difference in
409   hot plate performance was identified only in males. Although such differences could reflect sexual dimorphism, it is difficult to draw such a
410   conclusion as definitive for two major reasons: (i) in some tests where a significant difference in performance was observed for one gender, the
411   opposite gender may display a similar tendency, which remained non statistically significant; (ii) if for example females would be more prone to
412   effects of Gbx1 mutation we could expect to find them less performant in different tests; however, the gender effects were inconsistent and
413   concerned males or females depending on the measured parameter.

414   The spinal cord dorsal horn largely consists of inhibitory (GABAergic) and excitatory (glutamatergic) neurons that modulate somatosensory
415   inputs from the periphery, including pain, temperature and mechanoception (Glasgow, 2005). Our analysis of major neuronal classes revealed a
416   reduced proportion of GABAergic inhibitory interneurons expressing *Gad67* in the superficial dorsal horn of *Gbx1*-/- mice. Gbx1 may therefore
417   be functionally required for the differentiation of local inhibitory interneurons in the dorsal horn, corroborating a previous report of *Gbx1*
418   expression in a specific subset of GABAergic neurons in this region of the spinal cord (John, Wildner & Britsch 2005). Furthermore,

419 our findings suggest that *Gbx1* functions as a gene that promotes GABAergic over glutamatergic differentiation in the dorsal horn.

420 A disruption in the balance between inhibitory and excitatory neuronal activity could explain the phenotype observed in *Gbx1*

421 mutants. Indeed, the imbalance of inhibitory and excitatory activity may lead to altered signaling to second-order neurons in the

422 intermediate zone, which through an excitatory polysynaptic chain excite motor neurons in ventral horn to initiate protective

423 movements or abnormal proprioceptive behaviors. Such abnormal sensory processing is suggested at least for thermal stimuli, as

424 *Gbx1* mutant males displayed increased latency suggesting reduced pain in the hot plate test (thermosensory functions).

425 Finally, considering that locomotor deficits become apparent at P16-17, we cannot exclude that abnormal gait may result from postnatal

426 developmental or neurodegenerative events, which would need to be investigated.

427 Despite the clear behavioral phenotype and reduced pool of GABAergic neurons in the dorsal horn, we did not observe any change in the

428 expression of homeodomain factors involved in dorsal spinal cord patterning, or markers for primary sensory afferents, indicating that the

429 development of the dorsal horn is not profoundly affected in *Gbx1-/-* mutants. An explanation for these results—and for the overall mild

430 phenotype of the mutants—is that *Gbx1* and *Gbx2* are coexpressed in dorsal spinal cord cells at early stages of embryogenesis : hence the presence

431 of Gbx2 (and its subtle upregulation observed at E12.5-E14.5 in mutants) might compensate for Gbx1 loss of function with respect to early

432 regulatory events. Generation of *Gbx1*;*Gbx2* double mutants will be required to assess possible redundant functions, and the availability of a *Gbx2*

433 floxed (conditional) allele does allow strategies for a spinal cord-specific inactivation, which would alleviate the lethality of the *Gbx2* null mutants

434 (Wassarman *et al.* 1997).

435 Despite the importance of dorsal spinal cord in normal sensory processing, our knowledge concerning the establishment of neuronal circuits

436 remains limited (Graham, Brichta & Callister 2007; Todd 2010). In this regard, our work contributes to understand how transcription factors

437 cooperate for regulating cell specification and eventual distribution of neuronal subtypes in the developing spinal cord, providing clues for further

438 dissecting functional circuitry of the dorsal spinal cord.

Acknowledgments

440 We thank B. Schuhbaur for excellent technical assistance. We are grateful to Dr. K. Niederreither

441 for a critical reading of the manuscript, and to Drs. V. Brault, M. Paschaki and D. Dembélé for

442 help with statistical analysis. We thank Drs. C. Birchmeier, S. Britsch, F. Chen, K. Jagla, P.

443 Bouillet, B. Giros, P. Gruss, M. Tessier-Lavigne, R. Krumlauf and F. Rijli for the gift of reagents.

444 **Figure Legends**

445 **Figure 1.** Inactivation of the mouse *Gbx1* gene by homologous recombination in embryonic stem (ES) cells. (**A**) The upper
446 drawing shows the restriction map of the wild-type locus, boxes and lines corresponding to exons and introns, respectively. The
447 homeodomain sequence is in red. In the targeting vector (below), two *Gbx1* genomic fragments (between the dashed lines) flank a
448 *lacZ* reporter gene and the neomycin resistance gene (grey box), transcribed in the same orientation (thin arrow) as *Gbx1*. In the
449 recombined locus (lower drawing), 313 bp of *Gbx1* exon 2 (including the homeodomain) are replaced by the *lacZ neo* sequence.
450 The location of the 3' probe used for Southern blot analysis of ES cells is indicated in blue, and the PCR primers used to
451 distinguish wild-type and recombined alleles for genotyping of animals (F1, R1, LacZ R2; see Materials and methods) are also
452 indicated. (**B**) Southern blot analysis of a targeted cell line (+/-) in comparison to wild-type (+/+) HM-1 ES cells, using a probe
453 external to the targeting vector 3' homology arm. (**C**) Genotyping of wild-type (+/+), heterozygous (+/-) or homozygous mutant
454 (-/-) mice by PCR amplification of fragments specific for the wild-type (354 bp) or mutated allele (269 bp), using the F1, R1 and
455 LacZ R2 primers. (**D,E**) Anti-Gbx1 immunostaining. At E18.5, Gbx1 protein is absent in the spinal cord of *Gbx1-/-* mice (E), compared to wild- type (D). Scale bars: 100
456 µm.

457 **Figure 2.** Abnormal phenotype of a 10 week-old *Gbx1-/-* mouse when walking. Sequential pictures compare the normal gait of a wild-type mouse
458 (**A**) and the abnormal gait ("duck-like" walk) of a *Gbx1-/-* mutant when walking (**B**). A movie of these mice is available (Supplementary Movie).

459 **Figure 3**. Effects of *Gbx1* mutation on the latency and number of slips in the beam walking test. ** $p<0.01$ vs WT; Student t-test.

460 **Figure 4**. Open field performance of wild-type (WT) and *Gbx1-/-* mice. The distance traveled over the 20 min period of test reflects locomotor
461 activity. The average speed was calculated during movement in the whole arena for the entire period of testing. Exploration of the central part of
462 the open fied is expressed as the number of entries and percentage of time spent in the center. * $p<0.05$ and ** $p<0.01$ vs WT; Student t-test.

463 **Figure 5**. Startle reactivity and pre-pulse inhibition in wild-type (WT) and *Gbx1-/-* mice. Startle reactivity to background noise (65 dB), or to 70,
464 80, 85, 90 dB acoustic stimulation, and startle reflex to a 110 dB stimulus, are presented. The percentage of pre-pulse inhibition of the startle
465 response is displayed as a percentage of the pre-pulse intensity. WN, white noise; P, acoustic pulse intensity; ST, acoustic startle to 110 dB; PP,
466 pre-pulse intensity.

467 **Figure 6.** Absence of morphological and molecular abnormalities in the developing dorsal horn of *Gbx1-/-* mice. Sections through the spinal cord
468 of wild-type (A,C,E,G) and *Gbx1-/-* (B,D,F,H) mice at E18.5 (A,B) and E16.5 (C-H) are shown. All sections are at the lumbar level. (**A,B**) Nissl-
469 stained sections. No differences are detectable between wild-type and mutants (n=3). In situ hybridizations for two transcription factor encoding genes, *Lbx1*
470 (**C,D**) and *Lmx1b* (**E,F**), and for the axon guidance molecule netrin-1 (**G,H**), are shown (n=3 for each marker). No differences are observed between
471 wild-type and mutants. Scale bars: 100 µm.

472 **Figure 7.** Developmental progression of afferent projections in the dorsal horn of *Gbx1-/-* mice. (**A-B'**) Anti-calbindin-D28K antibody staining. At E18.5, calbindin fibers have
473 already entered the spinal gray matter in wild-type (A,A') and *Gbx1-/-* specimens (B,B'; n=3). Panels A',B' are higher magnifications of the areas boxed in A,B. (**C,D**) Expression of
474 *Drg11* in wild-type at E18.5 (C) and *Gbx1* mutant (D) mice. Mutant specimens were indistinguishable from wild-types (n=3). (**E-H**) Anti-peripherin antibody staining at E18.5
475 (E,F) and E16.5 (G,H). This staining reveals similar ingrowth of group IA muscle sensory afferents that grow to the ventral spinal cord (arrows) in wild-type (E,G) and mutant (F,H)
476 (n=3 for each stage). Scale bars: 100 µm (A',B': 50 µm).

477 **Figure 8.** Abnormal GABAergic differentiation in *Gbx1-/-* mice. Expression of *Gad67* in wild-type (**A,C**) and *Gbx1-/-* (**B,D**) mice at E18.5 (n=3).
478 Higher magnification views (C,D; areas boxed in A,B) show the dorsal horn, in which cell countings were performed. Expression of *Pax2* in wild-
479 type (**E**) and *Gbx1-/-* (**F**) mice at E18.5 (n=3). Expression of *Slc17a6* in wild-type (**G**) and *Gbx1-/-* (**H**) mice at E18.5 (n=3). (**I**) Countings
480 (percentages of labelled vs total cells) revealed that the proportion of Gad67+ cells is diminished by 16% in *Gbx1-/-* mice (50.89%±2.61 *Gad67+*

481   cells in WT; 34.85%±1.84 in *Gbx1-/-* mice; Genotype F(1,4)=223.85, ***p<0.001, Sections F(2,8)=2.22, NS, Genotype*Sections F(2,8)=1.23,

482   NS). Also, the proportion of Pax2+ cells is diminished by 14.7% in *Gbx1-/-* mice (58.57%±4,03 *Pax2+* cells in WT; 42.41%±5.96 in *Gbx1-/-*

483   mice; Genotype F(1,4)=449.36, ***p<0.001, Sections F(2,8)=3.34, NS, Genotype*Sections F(2,8)=6.3, p<0.05). In contrast, countings revealed

484   that the proportion of *Slc17a6+* cells is increased by 14.4% in *Gbx1-/-* mice (50.96%±1.84 *Slc17a6+* cells in WT; 65.16%±2.94 in *Gbx1-/-* mice;

485   Genotype F(1,4)=688.84, ***p<0.001, Sections F(2,8)=1.004, NS, Genotype*Sections F(2,8)=4.73, p<0.05). Scale bars: 100 µm.

486   **Figure 9**. Examples of TUNEL labeling of lumbar spinal cord sections of wild-type (A,C) and *Gbx1-/-* (B,D) mice. Sections are shown at E12.5 (A,B) (n=3) and

487   E18.5 (C,D) (n=3). Some TUNEL-labelled cells are seen in the dorsal root ganglia (drg) and in the ventral spinal cord (magnified in upper insets) at

488   E12.5, in both wild-type and mutant. (E) Apoptotic cells in the interdigital mesenchyme of an E13.5 forelimb are shown as a positive control. Scale

489   bars: 100 µm.

490   **Supplementary figure legends**

491   **Figure S1.** Expression analysis of *Gbx2* in the developing spinal cord of *Gbx1* mutants. Sections through the spinal cord of wild-type (A,C,E,G) and *Gbx1-/-*

492   (B,D,F,H) mice are shown. All sections are at the lumbar level. In situ hybridizations for *Gbx2* were performed at different developmental stages:

493   E12.5 (A,B; n=2), E14.5 (C,D; n=2), E16.5 (E,F; n=3), and E18.5 (G,H; n=3). Scale bars: 100 µm.

494   **Figure S2.** Analysis of rhombomeric markers in *Gbx1-/-* embryos. Whole-mount in situ hybridizations of E9.5 embryos with 2 markers of prospective rhombomeres: *Hoxb1,* which

495   labels rhombomere 4 (A,B; n=3), and *Hoxa2*, which marks rhombomeres 2 to 6 and associated neural crest (C,D; n=3). Scale bars: 50 µm.

496   **Figure S3.** In situ hybridization analysis of *Gad67*-expressing cells in the prenatal hindbrain. Sections are shown at various levels of the brain stem (A-F) and

497   cerebellum (G,H) of wild-type (A,C,E,G; n=3) and *Gbx1-/-* (B,D,F,H; n=3) mice at E18.5. Scale bars: 100 µm.

498   **Figure S4.** Analysis of developing spinal cord motor neurons in *Gbx1* mutants. Expression of Islet1 in the lumbar spinal cord of wild-type (A,C) and *Gbx1-/-*

499   (B,D) mice at E14.5 (A,B; n=3) and E16.5 (C,D; n=3). (E) Countings revealed that the numbers of Islet1+ cells in the ventral horn are not

500   significantly diminished in *Gbx1-/-* mice (at E14.5: 76±7.33 Islet1+ cells in WT; 75.22±3.13 in *Gbx1-/-* mice; Genotype F(1,4)=0.27, NS, Sections

501   F(2,8)=0.18, NS, Genotype*Sections F(2,8)=0.27, NS; at E16.5: 22.38±5.96 Islet1+ cells in WT; 25.33±6.70 in *Gbx1-/-* mice; Genotype

502   F(1,4)=3.03, NS, Sections F(2,8)=4.73, p<0.05, Genotype*Sections F(2,8)=5.46, p<0.05). Scale bars: 100 µm.

503   **Supplementary material : movie**

504   Movie sequence showing 10 week-old *Gbx1+/+* and *Gbx1-/-* mice.

505   **Table Captions**

506   **Table 1**. Effects of *Gbx1* mutation on body weight, basic neurological reflexes, specific motor abilities and pain sensitivity. Mice were analyzed at

507   10 weeks of age. Statistically different parameters in wild-type vs mutants appear in bold. * p<0.05 and **p<0.01 vs wild-type; Student t-test.

508   **Table 2**. Effects of *Gbx1* mutation on sensory nerve conduction velocity. The sensory nerve conduction velocity was measured at the level of the

509   caudal nerve. The latency and the amplitude of gastrocnemius muscle response evoked by sciatic nerve stimulation were also recorded. * p<0.05

510   vs wild-type; Student t-test.

511   **Bibliography**

512   *Bellocchio, E.E., Reimer, R.J., Fremeau, R.T., & Edwards, R.H., (2000) Uptake of glutamate into*
513   *synaptic vesicles by an inorganic phosphate transporter.* Science, **289**, 957-60.
514   *Ben-Ari, Y., Gaiarsa, J.L., Tyzio, R.,& Khazipov, R. , (2007) GABA: a pioneer transmitter that*
515   *excites immature neurons and generates primitive oscillations.* Physiological Review, **87**, 1215-
516   84.
517   *Bermingham, N.A., Hassan, B.A., Wang, V.Y., Fernandez, M., Banfi, S., Bellen,*
518   *H.J., Fritzsch, B., &v Zoghbi, H.Y., (2001) Proprioceptor pathway development is*
519   *dependent on Math1.* Neuron, **30**, 411-22.

520   *Bouillet, P., Chazaud, C., Oulad-Abdelghani, M., Dollé, P., & Chambon, P., (1995) Sequence and expression pattern of the Stra7 (Gbx-2) homeobox-*
521   *containing gene induced by retinoic acid in P19 embryonal carcinoma cells.* Developmental Dynamics, **204**, 372-382.

522   *Briscoe, J., & Ericson, J., (1999) The specification of neuronal identity by graded*
523   *Sonic Hedgehog signalling.* Seminar Cell Developmental Biology, **10**, 353-62.

524   *Brown, A., (1981) Organisation in the spinal cord.* New York : Springer.

525   *Brown, S.D.M., Chambon, P., & Hrabé de Angelis, M., (2005) EMPReSS: standardized phenotype screens for functional*
526   *annotation of the mouse genome.* Nature Genetics, **37**, 1155.

527   *Buckley, D.M., Burroughs-Garcia, J., Lewandoski, M., & Waters, ST., (2013) Characterization of*
528   *the gbx1(-/-) mouse mutant: a requirement for gbx1 in normal locomotion and sensorimotor*
529   *circuit development.* PLoS One, **8**(2):e56214.
530   *Burroughs-Garcia, J., Sittaramane, V., Chandrasekhar, A., & Waters, S.T., (2011) Evolutionarily*
531   *conserved function of Gbx2 in anterior hindbrain development.* Developmental Dynamics, **240**,
532   828-38.

533   *Caspary, T., & Anderson, K.V., (2003) Patterning cell types in the dorsal spinal*
534   *cord: what the mouse mutants say.* Nature Reviews Neuroscience, **4**, 289-9.

535   *Chen, Z.F., Rebelo, S., White, F., Malmberg, A.B., Baba, H., Lima, D., Woolf, C.J.,*
536   *Basbaum, A.I., & Anderson, D.J., (2001) The paired homeodomain protein DRG11*
537   *is required for the projection of cutaneous sensory afferent fibers to the dorsal*
538   *spinal cord.* Neuron, **31**, 59-73.
539   *Cheng, L., Arata, A., Mizuguchi, R., Qian, Y., Karunaratne, A., Gray, P.A., Arata, S., Shirasawa,*
540   *S., Bouchard, M., Luo, P., Chen, C.L., Busslinger, M., Goulding, M., Onimaru, H., & Ma, Q.,*
541   (2004) *Tlx3 and Tlx1 are post-mitotic selector genes determining glutamatergic over GABAergic*
542   *cell fates.* Nature Neuroscience, **7**, 510-7.
543   *Chiang, C., Young, K.E., & Beachy, P.A., (1995) Control of Drosophila tracheal branching by the*
544   *novel homeodomain gene unplugged, a regulatory target for genes of the bithorax complex.*
545   Development, **121**, 3901-12.
546   *Chotteau-Lelièvre, A., Dollé, P., & Gofflot F., (2006) Expression analysis of murine genes using*
547   *in situ hybridization with radioactive and nonradioactively labeled RNA probes.* Methods
548   Molecular Biology, **326**, 61-87.

549 *Cui, X., & Doe, C.Q.,* (1995) *The role of the cell cycle and cytokinesis in regulating neuroblast*
550 *sublineage gene expression in the Drosophila CNS.* Development, 121, 3233-43.
551 *Dickenson, A.H.,* (2002) *Gate control theory of pain stands the test of time.* British Journal of
552 Anaesthia, **88**, 755-7.

553 *Escurat, M., Djabali, K., Gumpel, M., Gros, F., & Portier, M.M., (*1990) *Differential*
554 *expression of two neuronal intermediate-filament proteins,*
555 *peripherin and the low-molecular-mass neurofilament protein*
556 *(NF-L), during the development of the rat.* Journal of Neuroscience, **10**, 764-
557 84.

558 *Fremeau, R.T., Troyer, M.D., Pahner, I., Nygaard, G.O., Tran, C.H., Reimer, R.J., Bellocchio,*
559 *E.E., Fortin, D., Storm-Mathisen, J., & Edwards, R.H.,* (2001) *The expression of vesicular*
560 *glutamate transporters defines two classes of excitatory synapse.* Neuron, **31**, 247-60.
561 *Glasgow, S. M.,* (2005) *Ptf1a determines GABAergic over glutamatergic neuronal cell fate in the spinal cord dorsal*
562 *horn.* Development, **132**, 5461-5469.

563 *Goulding, M., Lanuza, G., Sapir, T., & Narayan, S.,* (2002) *The formation of*
564 *sensorimotor circuits.* Current Opinion Neurobiology, **12**, 508-15.

565 *Gowan, K., Helms, A.W., Hunsaker, T.L., Collisson, T., Ebert, P.J., Odom, R., &*
566 *Johnson, J.E.,* (2001). *Crossinhibitory activities of Ngn1 and Math1 allow*
567 *specification of distinct dorsal interneurons.* Neuron, **31**, 219-32.

568 *Graham, B.A., Brichta, A.M., & Callister, R.J.,* (2007) *Moving from an averaged to specific*
569 *view of spinal cord pain processing circuits.* Journal of Neurophysiology, **98**, 1057-63.
570 *Gross, M.K., Dottori, M., & Goulding, M.,* (2002) *Lbx1 specifies somatosensory*
571 *association interneurons in the dorsal spinal cord.* Neuron, **16**, 535-49.

572 *Guo, Z., Zhao, C., Huang, M., Huang, T., Fan, M., Xie, Z., Chen, Y., Zhao, X.,*
573 *Xia, G., Geng, J., & Cheng, L.,* (2012) *Tlx1/3 and Ptf1a control the expression of*
574 *distinct sets of transmitter and peptide receptor genes in the developing dorsal*
575 *spinal cord.* Journal of Neuroscience, **32**, 8509-20.

576 *Hatcher, J.P., Jones, D.N.C., Rogers, D.C., Hatcher, P.D., Reavill, P.D., Hagan, J.J., & Hunter, A.J.,* (2001) *Development of*
577 *SHIRPA to characterize the phenotype of gene-targeted mice.* Behaviour Brain Research, **125**, 43-47.

578 *Helms, A.W., & Johnson, J.E.,* (2003) *Specification of dorsal spinal cord*
579 *interneurons.*
580 Current Opinion Neurobiology, **13**, 42-9.

581 *Honda, CN.,* (1995) *Differential distribution of calbindin-D28k and parvalbumin in*
582 *somatic and visceral sensory neurons.* Neuroscience, **68**, 883-92.

583   *Hu, J., Huang, T., Li, T., Guo, Z., & Cheng, L.* (2012) *cMaf Is Required for the Development of Dorsal Horn*
584   *Laminae III/IV Neurons and Mechanoreceptive DRG Axon Projections.* Journal of Neuroscience, **32**, 5362-5373.

585   *Irwin, S.,* (1968) *Comprehensive observational assessment: Ia. A systematic, quantitative procedure for assessing the behavioral*
586   *and physiologic state of the mouse.* Psychopharmacologia, **13**, 222-257.

587   *John, A., Wildner, H., & Britsch, S.,* (2005) *The homeodomain transcription factor*
588   *Gbx1 identifies a subpopulation of late-born GABAergic interneurons in the*
589   *developing dorsal spinal cord.* Developmental Dynamics, **234**, 767-71.
590   *Kaneko, T,& Fujiyama, F.,* (2002) *Complementary distribution of vesicular glutamate*
591   *transporters in the central nervous system.* Neuroscience Research, **42**, 243-50.
592   *Larsson, M., & Broman, J.,* (2011) *Synaptic plasticity and pain: role of ionotropic*
593   *glutamate receptors.* Neuroscientist, **17**, 256-73.

594   *Lee, K.J., & Jessell, T.M.,* (1999) *The specification of dorsal cell fates in the*
595   *vertebrate central nervous system.* Annual Reviews Neuroscience, **22**, 261-94.

596   *Leonardo, E.D., Hinck, L., Masu, M., Keino-Masu, K., Fazeli, A., Stoeckli, E.T.,*
597   *Ackerman, S.L., Weinberg, R.A., & Tessier-Lavigne, M.,* (1997) *Guidance of*
598   *developing axons by netrin-1 and its receptors.* Cold Spring Harb Symp Quant Biol, **62**,
599   467-78.

600   *Le Mouellic, H., Lallemand, Y., & Brûlet, P.,* (1990) *Targeted replacement of the*
601   *homeobox gene Hox-3.1 by the Escherichia coli lacZ in mouse*
602   *chimeric embryos.* Proceedings of the National Academy of Sciences U S A , **87**, 4712-6.

603   *Lewis, K.E.,* (2006) *Do genes regulate simple behaviours? Understanding how*
604   *different neurons in the vertebrate spinal cord are genetically specified.* Philosophical
605   Transactions of the Royal Society London B Biological Science, **361**, 45-66.

606   *Lin, X., Swaroop, A., Vaccarino, F.M., Murtha, M.T., Haas, M., Ji, X., Ruddle, F.H., & Leckman, J.F.,* (1996) *Characterization and sequence analysis of the*
607   *human homeobox-containing gene GBX2.* Genomics, **31**, 335-342.
608   *Malcangio, M., & Bowery, N.G.,* (1996) *GABA and its receptors in the spinal cord.* Trends in
609   Pharmacological Sciences, **17**, 457-62.
610   *Magin, T.M., McWhir, J., & Melton, D.W.,* (1992) *A new mouse embryonic stem*
611   *cell line with good germ line contribution and gene targeting frequency.* Nucleic
612   Acids Research, **20**, 3795-6.

613   *Melzack, R., & Wall, P.D.,* (1965) *Pain mechanisms: a new theory.* Science, **150**, 971-9.
614   *Müller, T., Brohmann, H., Pierani, A., Heppenstall, P.A., Lewin, G.R., Jessell, T.M.,*
615   *& Birchmeier, C.,* (2002) *The homeodomain factor lbx1 distinguishes*
616   *two major programs of neuronal differentiation in the dorsal*

617 *spinal cord*. Neuron, **34**, 551-62.

618 *Nagy, A., Gertsenstein, M., Vintersten, K., & Behringer, R.*, (2003) *Manipulating the Mouse*
619 *Embryo: A Laboratory Manual*. Cold Spring Harbor Laboratory Press, New York.

620 *Niss, K., & Leutz, A.*, (1998) *Expression of the homeobox gene GBX2 during chicken development*. Mechanisms of Development, **76**, 151-155.

621 *Ozaki, S., & Snider, W.D.*, (1997) *Initial trajectories of sensory axons*
622 *toward laminar targets in the developing mouse spinal cord.*
623 Journal of Comparative Neurology, **380**, 215-29.

624 *Rexed, B.*, (1952) *The cytoarchitectonic organization of the spinal cord in the cat.*
625 Journal of Comparative Neurology, **96**, 414-95.

626 *Ramírez-Solis, R., Davis, A.C., & Bradley, A.*, (1993) *Gene targeting in embryonic*
627 *stem cells.* Methods Enzymology, **225**, 855-78.

628 *Rebelo, S., Reguenga, C., Lopes, C., & Lima, D.*, (2010). *Prrxl1 is required for the generation of*
629 *a subset of nociceptive glutamatergic superficial spinal dorsal horn neurons.* Developmental
630 Dynamics, **239**, 1684-94.
631 *Rhinn, M., & Brand, M.*, (2001) *The midbrain-hindbrain boundary organizer.* Current Opinion
632 Neurobiology, **11**, 34-42.
633 *Rhinn, M., Lun, K., Amores, A., Yan, Y.L., Postlethwait, J.H., & Brand, M.*, (2003) *Cloning,*
634 *expression and relationship of zebrafish gbx1 and gbx2 genes to Fgf signaling.* Mechanisms of
635 Development, **120**, 919-36.

636 *Rhinn, M., Lun, K., Werner, M., Simeone, A., & Brand, M.,* (2004) *Isolation and*
637 *expression of the homeobox gene Gbx1 during mouse development.* Developmental
638 Dynamics, **229**, 334-9.
639 *Rhinn, M., Lun, K., Ahrendt, R., Geffarth, M., & Brand, M.*, (2009) *Zebrafish gbx1 refines the*
640 *midbrain-hindbrain boundary border and mediates the Wnt8 posteriorization signal.* Neural
641 Development, **2**, 4-12.
642 *Robertson, E. J.*, (1987). *Embryo-derived stem cell lines*. In *Teratocarcinomas and Embryonic*
643 *Stem Cells : a Practical Approach*. (ed. E. J. Robertson). Oxford, England: IRL Press. pp. 71-112.
644 *Shamim, H., & Mason, I.*, (1998) *Expression of Gbx-2 during early development of the chick embryo*. Mechanisms of Development, **76**, 157-159.
645 *Simeone, A.,* (2000) *Positioning the isthmic organizer where Otx2 and Gbx2 meet.* Trends in
646 Genetics, **16** , 237-40.
647 *Somogyi, R., Wen, X., Ma, W., & Barker, J.L.*, (1995) *Developmental kinetics of GAD family*
648 *mRNAs parallel neurogenesis in the rat spinal cord.* Journal of Neuroscience, **15**, 2575-91.

649 *Todd, A.J.,* (2010) *Neuronal circuitry for pain processing in the dorsal horn.* Nature
650 Reviews Neuroscience, **11**, 823-36.

651 *Wassarman, K.M., Lewandoski, M., Campbell, K., Joyner, A.L., Rubenstein, J.L.,*
652 *Martinez, S., & Martin, G.R.*, (1997) *Specification of the anterior hindbrain and*

653 *establishment of a normal mid/hindbrain organizer is dependent on Gbx2 gene*
654 *function.* Development, **124**, 2923-3.

655 *Waters, S.T., Wilson, C.P., & Lewandoski, M.,* (2003) *Cloning and embryonic*
656 *expression analysis of the mouse Gbx1 gene.* Gene Expression Patterns, **3**, 313-7.

657 *Waters, S.T., & Lewandoski, M.,* (2006) *A threshold requirement for Gbx2 levels in hindbrain*
658 *development.* Development, **133**,1991-2000.
659 *White, F.A., Keller-Peck, C.R., Knudson, C.M., Korsmeyer, S.J., and Snider, W.D.* (1998*)*
660 *Widespread elimination of naturally occurring neuronal death in Bax-deficient mice.* Journal of
661 Neuroscience, **18**,1428-39.
662 *Willis, W., & Coggeshall, R.E.,* (1991) Sensory mechanisms of the spinal cord. Plenum Press, NY.

Effects of *Gbx1* mutation on body weight, basic neurological reflexes, specific motor abilities and pain sensitivity.

Mice were analyzed at 10 weeks of age. Statistically different parameters in wild-type vs mutants appear in bold. * p<0.05 and **p<0.01 vs wild-type; Student t-test.

1 **Table 1:**

	Males		Females	
	Wild-type	*Gbx1-/-*	**Wild-type**	*Gbx1-/-*
Body weight (g)	26.57 ± 0.73	25.40 ± 0.48	19.81 ± 0.32	20.88 ± 0.89
Gait (% abnormal)	0	**43%****	0	**63%****
Short-term locomotor activity (number of squares crossed in 30 s)	26.70 ± 1.37	**19.71 ± 1.39****	28.33 ± 1.00	**22.00 ± 1.57****
Rotarod- 4 to 40 rpm in 5 min (s)	123.87 ± 17.56	95.11 ± 15.08	116.33 ± 9.10	130.25 ± 14.99
Grip strength (adjusted to body weight) (g) *2 paws*	3.97 ± 0.18	4.00 ± 0.24	3.75 ± 0.17	3.38 ± 0.26
4 paws	8.30 ± 0.24	7.72 ± 0.37	7.00 ± 0.24	7.22 ± 0.54
Hot plate (s)	13.43 ± 1.26	**17.13 ± 1.08***	12.72 ± 1.15	15.03 ± 1.63

Effects of *Gbx1* mutation on sensory nerve conduction velocity.

The sensory nerve conduction velocity was measured at the level of the caudal nerve. The latency and the amplitude of gastrocnemius muscle response evoked by sciatic nerve stimulation were also recorded. * p<0.05 vs wild-type; Student t-test.

2 **Table 2 :**

		Males		Females	
		Wild-type	*Gbx1*-/-	**Wild-type**	*Gbx1*-/-
Sensory nerve conduction velocity (m/s)		70.33 ± 1.70	72.20 ± 1.53	63.93 ± 2.35	**71.81 ± 1.50***
Gastrocnemius M-wave	*Latency (ms)*	0.93 ± 0.06	0.91 ± 0.06	0.99 ± 0.08	0.84 ± 0.05
	Amplitude (mV)	43.99 ± 3.15	44.60 ± 5.87	46.46 ± 6.70	55.41 ± 6.03

Figure 1

Inactivation of the mouse *Gbx1* gene by homologous recombination in embryonic stem (ES) cells.

(A) The upper drawing shows the restriction map of the wild-type locus, boxes and lines corresponding to exons and introns, respectively. The homeodomain sequence is in red. In the targeting vector (below), two *Gbx1* genomic fragments (between the dashed lines) flank a *lacZ* reporter gene and the neomycin resistance gene (grey box), transcribed in the same orientation (thin arrow) as *Gbx1*. In the recombined locus (lower drawing), 313 bp of *Gbx1* exon 2 **(**including the homeodomain) are replaced by the *lacZ neo* sequence. The location of the 3' probe used for Southern blot analysis of ES cells is indicated in blue, and the PCR primers used to distinguish wild-type and recombined alleles for genotyping of animals (F1, R1, LacZ R2; see Materials and methods) are also indicated. **(B)** Southern blot analysis of a targeted cell line (+/-) in comparison to wild-type (+/+) HM-1 ES cells, using a probe external to the targeting vector 3' homology arm. **(C)** Genotyping of wild-type (+/+), heterozygous (+/-) or homozygous mutant (-/-) mice by PCR amplification of fragments specific for the wild-type (354 bp) or mutated allele (269 bp), using the F1, R1 and LacZ R2 primers. **(D,E)** Anti-Gbx1 immunostaining. At E18.5, Gbx1 protein is absent in the spinal cord of *Gbx1-/-* mice (E), compared to wild- type (D). Scale bars: 100 μm.
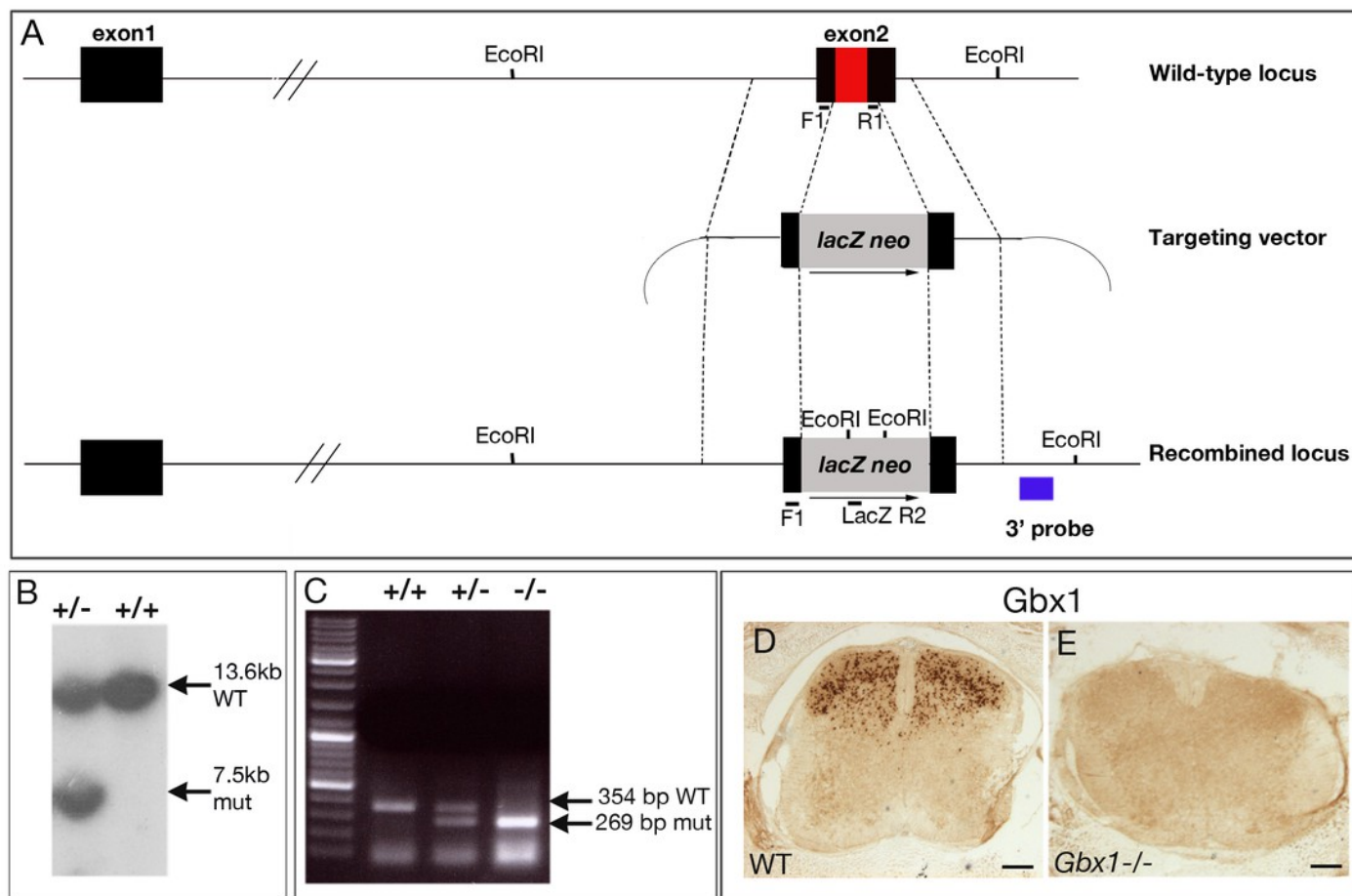
Figure 2

Abnormal phenotype of a *Gbx1-/-* mouse when walking.

Sequential pictures compare the normal gait of a wild-type mouse (**A**) and the abnormal gait ("duck-like" walk) of a *Gbx1-/-* mutant when walking (**B**). A movie of these mice is available (Supplementary Movie).
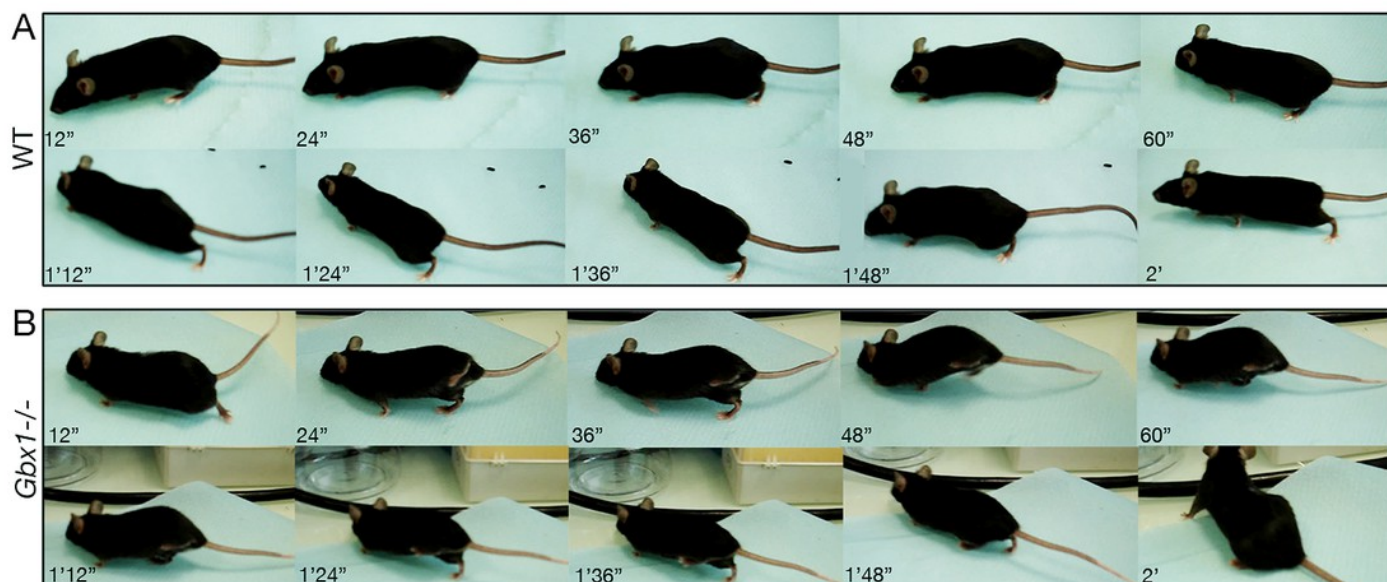
Figure 3

Effects of *Gbx1* mutation on the latency and number of slips in the beam walking test.

** p<0.01 vs WT; Student t-test.
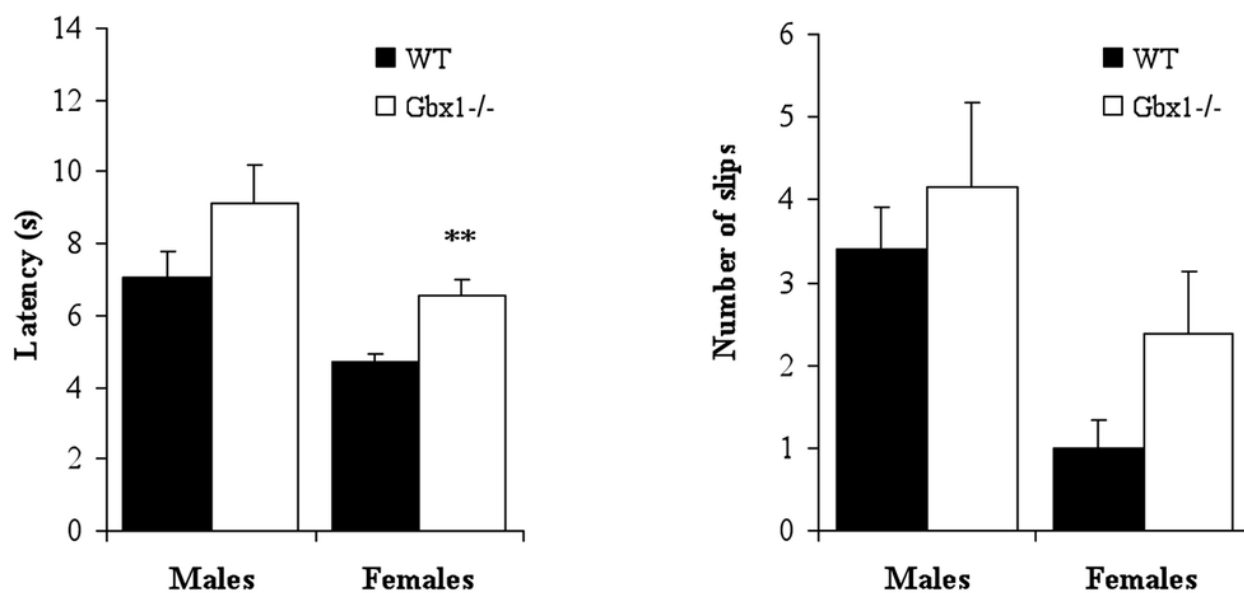
Figure 4

Open field performance of wild-type (WT) and *Gbx1-/-* mice.

The distance traveled over the 20 min period of test reflects locomotor activity. The average speed was calculated during movement in the whole arena for the entire period of testing. Exploration of the central part of the open fied is expressed as the number of entries and percentage of time spent in the center. * $p<0.05$ and ** $p<0.01$ vs WT; Student t-test.
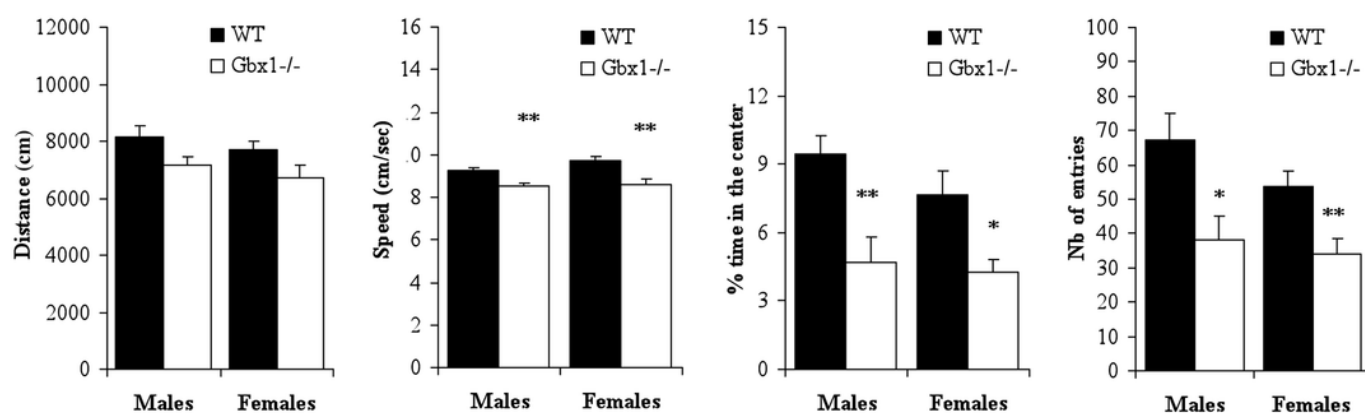
Figure 5

Startle reactivity and pre-pulse inhibition in wild-type (WT) and *Gbx1-/-* mice.

Startle reactivity to background noise (65 dB), or to 70, 80, 85, 90 dB acoustic stimulation, and startle reflex to a 110 dB stimulus, are presented. The percentage of pre-pulse inhibition of the startle response is displayed as a percentage of the pre-pulse intensity. WN, white noise; P, acoustic pulse intensity; ST, acoustic startle to 110 dB; PP, pre-pulse intensity.
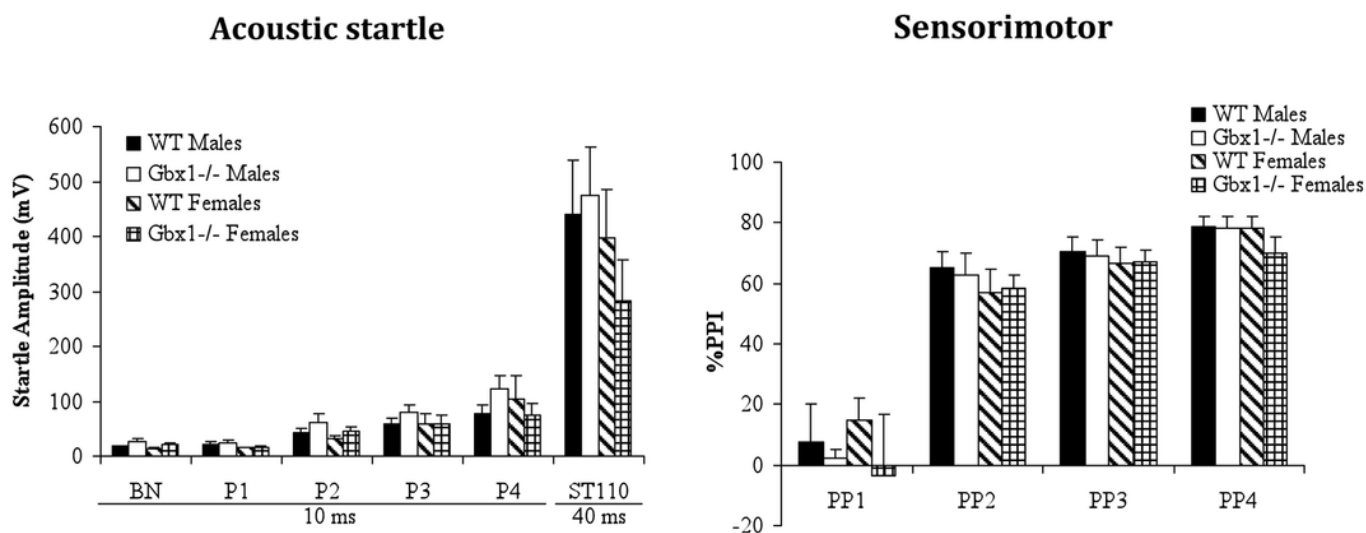
Figure 6

Absence of morphological and molecular abnormalities in the developing dorsal horn of *Gbx1-/-* mice.

Sections through the spinal cord of wild-type (A,C,E,G) and *Gbx1-/-* (B,D,F,H) mice at E18.5 (A,B) and E16.5 (C-H) are shown. All sections are at the lumbar level. (**A,B**) Nissl-stained sections. No differences are detectable between wild-type and mutants (n=3). In situ hybridizations for two transcription factor encoding genes, *Lbx1* (**C,D**) and *Lmx1b* (**E,F**), and for the axon guidance molecule netrin-1 (**G,H**), are shown (n=3 for each marker). No differences are observed between wild-type and mutants. Scale bars: 100 μm.
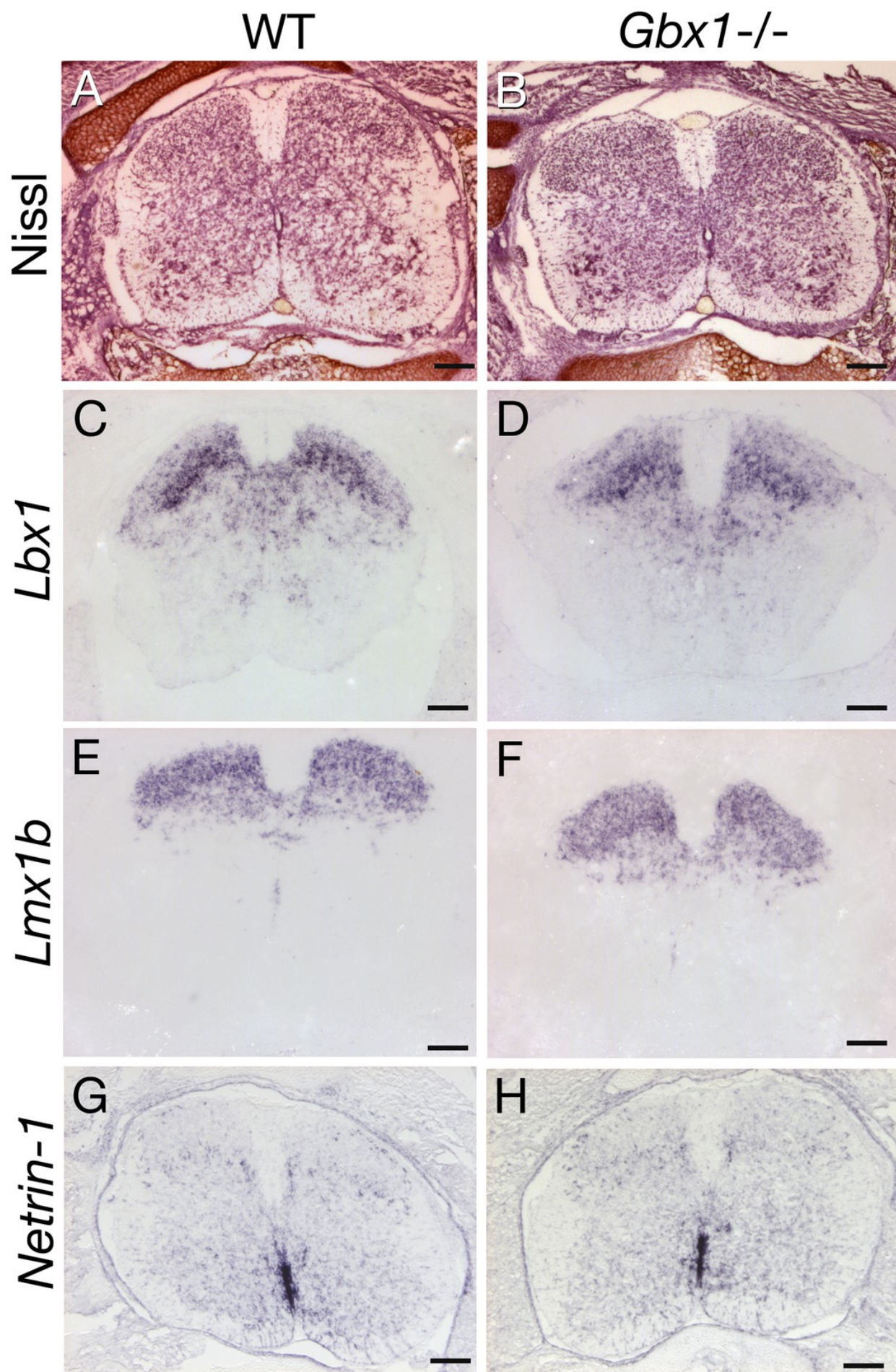
WT

Gbx1-/-

Figure 7

Developmental progression of afferent projections in the dorsal horn of *Gbx1-/-* mice.

(**A-B'**) Anti-calbindin-D28K antibody staining. At E18.5, calbindin fibers have already entered the spinal gray matter in wild-type (A,A') and *Gbx1-/-* specimens (B,B'; n=3). Panels A',B' are higher magnifications of the areas boxed in A,B. (**C,D**) Expression of *Drg11* in wild-type at E18.5 (C) and *Gbx1* mutant (D) mice. Mutant specimens were indistinguishable from wild-types (n=3). (**E-H**) Anti-peripherin antibody staining at E18.5 (E,F) and E16.5 (G,H). This staining reveals similar ingrowth of group IA muscle sensory afferents that grow to the ventral spinal cord (arrows) in wild-type (E,G) and mutant (F,H) (n=3 for each stage). Scale bars: 100 μm (A',B': 50 mm).
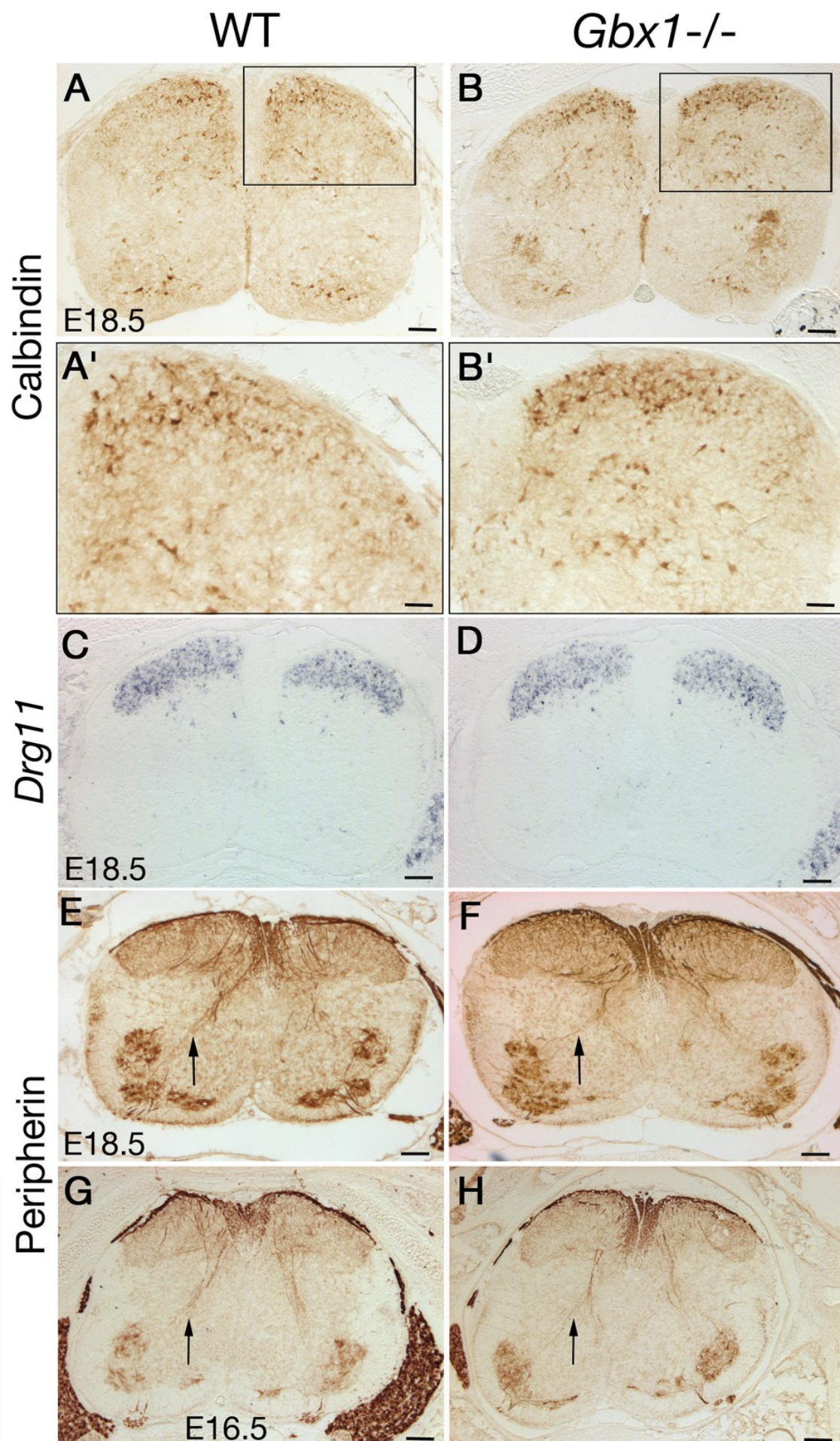
Figure 8

Abnormal GABAergic differentiation in *Gbx1-/-* mice.

Expression of *Gad67* in wild-type (**A,C**) and *Gbx1-/-* (**B,D**) mice at E18.5 (n=3). Higher magnification views (C,D; areas boxed in A,B) show the dorsal horn, in which cell countings were performed. Expression of *Pax2* in wild-type (**E**) and *Gbx1-/-* (**F**) mice at E18.5 (n=3). Expression of *Slc17a6* in wild-type (**G**) and *Gbx1-/-* (**H**) mice at E18.5 (n=3). (**I**) Countings (percentages of labelled vs total cells) revealed that the proportion of Gad67+ cells is diminished by 16% in *Gbx1-/-* mice (50.89% ±2.61 *Gad67*+ cells in WT; 34.85%±1.84 in *Gbx1-/-* mice; Genotype $F_{(1,4)}$=223.85, ***$p<0.001$, Sections $F_{(2,8)}$=2.22, NS, Genotype*Sections $F_{(2,8)}$=1.23, NS). Also, the proportion of Pax2+ cells is diminished by 14.7% in *Gbx1-/-* mice (58.57%±4,03 *Pax2*+ cells in WT; 42.41%±5.96 in *Gbx1-/-* mice; Genotype $F_{(1,4)}$=449.36, ***$p<0.001$, Sections $F_{(2,8)}$=3.34, NS, Genotype*Sections $F_{(2,8)}$=6.3, $p<0.05$). In contrast, countings revealed that the proportion of *Slc17a6*+ cells is increased by 14.4% in *Gbx1-/-* mice (50.96%±1.84 *Slc17a6*+ cells in WT; 65.16%±2.94 in *Gbx1-/-* mice; Genotype $F_{(1,4)}$=688.84, ***$p<0.001$, Sections $F_{(2,8)}$=1.004, NS, Genotype*Sections $F_{(2,8)}$=4.73, $p<0.05$). Scale bars: 100 µm.
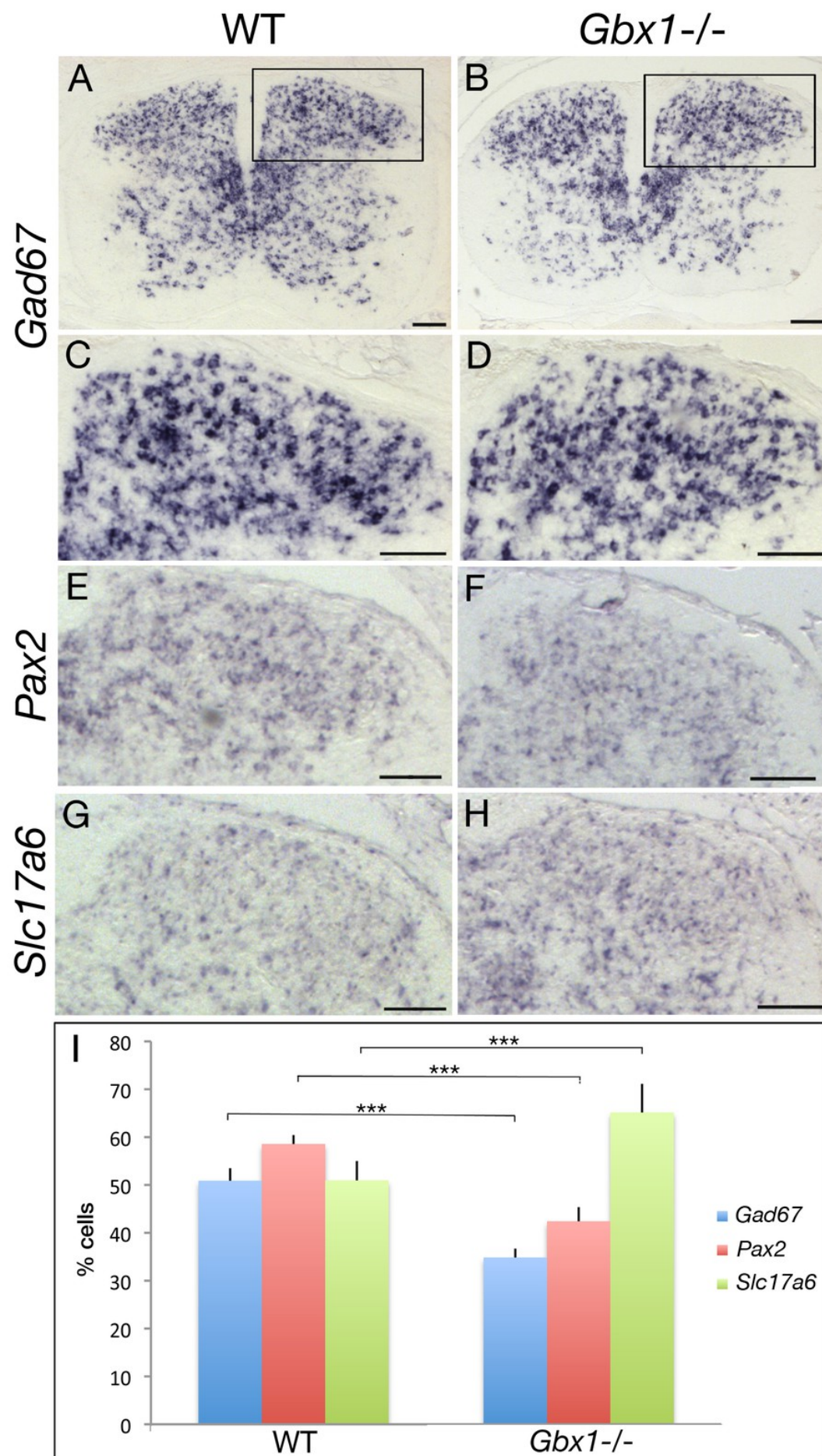
Figure 9

Examples of TUNEL labeling of lumbar spinal cord sections of wild-type (A,C) and *Gbx1-/-* (B,D) mice.

Sections are shown at E12.5 (A,B) (n=3) and E18.5 (C,D) (n=3). Some TUNEL-labelled cells are seen in the dorsal root ganglia (drg) and in the ventral spinal cord (magnified in upper insets) at E12.5, in both wild-type and mutant. (E) Apoptotic cells in the interdigital mesenchyme of an E13.5 forelimb are shown as a positive control. Scale bars: 100 μm.